Imprint of SUSY in radiative B meson decays

K. Hidaka
Tokyo Gakugei University

Collaboration with
H. Eberl, E. Ginina (HEPHY, Vienna),
A. Ishikawa (BELLE II, KEK, Tsukuba)

PPP2022, 29 Aug 2022, Kyoto, Japan

Contents

1. Introduction

- *We study **supersymmetric (SUSY) effects on $C_7(\mu_b)$ and $C'_7(\mu_b)$** which are the Wilson coefficients (WCs) for b -> s gamma at b-quark mass scale μ_b and are closely related to **radiative B meson decays**.*

- *The SUSY-loop contributions to the $C_7(\mu_b)$ and $C'_7(\mu_b)$ are calculated in the Minimal Supersymmetric Standard Model **(MSSM) with general quark flavor violation (QFV)**.*

- *In the computation of the WCs, **for the first time** we perform a systematic **MSSM parameter scan** respecting all the relevant theoretical and experimental constraints, such as those from K- & B-meson and H(125) data and recent limits on Supersymmetric (SUSY) particle masses from LHC experiments.*

- *Here we study a possibility that **imprint of SUSY** can be found in radiative B meson decays, focusing on the WCs $C_7(\mu_b)$ and $C'_7(\mu_b)$.*

2. _MSSM with QFV_

Key parameters in this study are:

* _QFV parameters:_ $\tilde{c}_{L/R} - \tilde{t}_{L/R}$ _&_ $\tilde{s}_{L/R} - \tilde{b}_{L/R}$ _mixing parameters_

* _QFC parameter:_ $\tilde{t}_L - \tilde{t}_R$ _&_ $\tilde{b}_L - \tilde{b}_R$ _mixing parameters_

$M^2{}_{Q23}$ = ($\tilde{c}_L - \tilde{t}_L$ _mixing parameter_)

$M^2{}_{U23}$ = ($\tilde{c}_R - \tilde{t}_R$ _mixing parameter_)

$M^2{}_{D23}$ = ($\tilde{s}_R - \tilde{b}_R$ _mixing parameter_)

T_{U23} = ($\tilde{c}_R - \tilde{t}_L$ _mixing parameter_)

T_{U32} = ($\tilde{c}_L - \tilde{t}_R$ _mixing parameter_)

T_{U33} = ($\tilde{t}_L - \tilde{t}_R$ _mixing parameter_)

T_{D23} = ($\tilde{s}_R - \tilde{b}_L$ _mixing parameter_)

T_{D32} = ($\tilde{s}_L - \tilde{b}_R$ _mixing parameter_)

T_{D33} = ($\tilde{b}_L - \tilde{b}_R$ _mixing parameter_)

3. *Constraints on the MSSM*

We respect the following experimental and theoretical constraints:

(1) *The recent LHC limits on the masses of squarks, sleptons, gluino, charginos and neutralinos.*

(2) *The constraint on $(m_{A/H+}, \tan\beta)$ from recent MSSM Higgs boson search at LHC.*

(3) *The constraints on the QFV parameters from the B & K meson data.*

$$B(b \rightarrow s\,\gamma) \qquad \Delta M_{Bs} \qquad B(B_s \rightarrow \mu^+\mu^-) \qquad B(B_u^+ \rightarrow \tau^+\nu) \;\; \textit{etc.}$$

(4) *The constraints from the observed Higgs boson mass and couplings at LHC ; e.g.*
 121.6 GeV < m_h^0 < 128.6 GeV (allowing for theoretical uncertainty) ,
 0.71 < κ_b < 1.43 (ATLAS),   0.56 < κ_b < 1.70 (CMS)

(5) *The experimental limit on SUSY contributions to the electroweak ρ parameter*
 $\Delta\rho$ (SUSY) < 0.0012.

(6) *Theoretical constraints from the vacuum stability conditions for the trilinear couplings $T_{U\alpha\beta}$ and $T_{D\alpha\beta}$.*

* _Constraints on the MSSM parameters from W boson mass data:_

The recent m_W data from CDF II [1] is quite inconsistent with the other experimental data. (-> See backup slides.)
[1] CDF Collaboration, Science 376, 170–176 (2022)

This issue of the m_W data is not yet settled.

Hence, we do not take into accont this m_W constraint on the MSSM parameters in our analysis.

4. *Parameter scan in the MSSM*

- *We compute the WCs $C_7(\mu_b)$ and $C'_7(\mu_b)$ at LO in the MSSM with QFV.*

- *We take parameter scan ranges as follows:*

$$1 \; TeV < \; M_{SUSY} \; < 5 \; TeV$$

$10 < tan\beta < 80$
$2500 < M_3 < 5000 \; GeV$
$100 \;\; < M_2 < 2500 \; GeV$
$100 \;\; < M_1 < 2500 \; GeV$
$100 \;\; < \mu < 2500 \; GeV$
$1350 < m_A(pole) < 6000 \; GeV$
etc. etc.

- *In the parameter scan, all of the relevant experimental and theoretical constraints are imposed.*

- *8660000 parameter points are generated and 72904 points survive the constraints.*

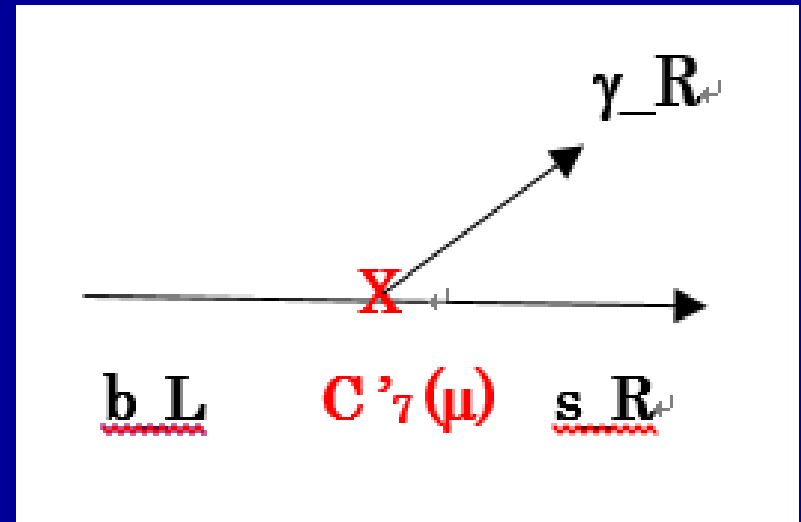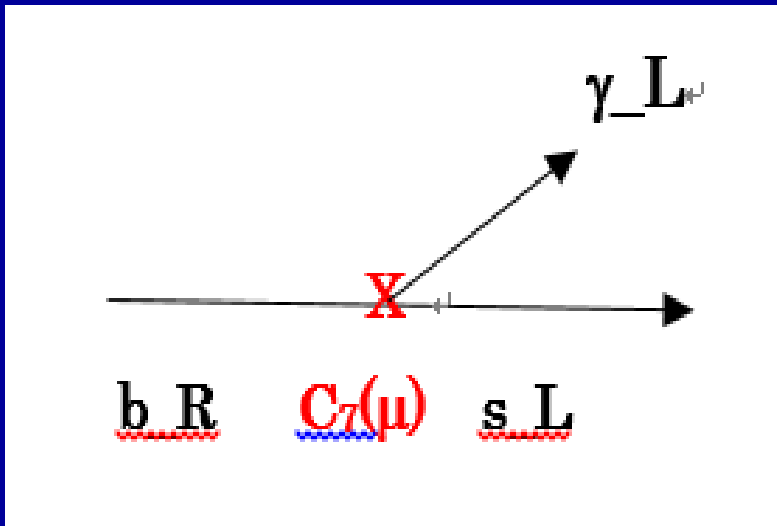# 5. *WC's $C_7(\mu_b)$ and $C'_7(\mu_b)$ in the MSSM with QFV*

Low-energy effective Hamiltonian, at the bottom mass scale μ_b :

$$\mathcal{H}_{eff} = -\frac{4G_F}{\sqrt{2}} V_{tb} V_{ts}^* \sum_i C_i(\mu_b) Q_i(\mu_b) \ .$$

$$Q_2 = \bar{s}_L \gamma_\mu c_L \bar{c}_L \gamma^\mu b_L \ ,$$

C_7
$$Q_7 = \frac{e}{16\pi^2} m_b \bar{s}_L \sigma^{\mu\nu} b_R F_{\mu\nu} \ ,$$

C_8
$$Q_8 = \frac{g_s}{16\pi^2} m_b \bar{s}_L \sigma^{\mu\nu} G^a_{\mu\nu} T_a b_R \ .$$

$$Q'_2 = \bar{s}_R \gamma_\mu c_R \bar{c}_R \gamma^\mu b_R \ ,$$

C'_7
$$Q'_7 = \frac{e}{16\pi^2} m_b \bar{s}_R \sigma^{\mu\nu} b_L F_{\mu\nu} \ ,$$

C'_8
$$Q'_8 = \frac{e}{16\pi^2} m_b \bar{s}_R \sigma^{\mu\nu} G^a_{\mu\nu} T_a b_L \ .$$

(Note) $C'_{7,\,8}(\mu) \approx 0$ *in SM*

- *We compute the WCs $C_7(\mu_b)$ and $C'_7(\mu_b)$ at b-quark mass scale μ_b at LO in the* *MSSM with QFV.*

- *The WCs $C_7(\mu_b)$ and $C'_7(\mu_b)$ can be measured precisely at* *BELLE II* *&* *LHCb-Upgrade**!*

We compute $C_{7,8}(\mu_W)$ and $C'_{7,8}(\mu_W)$ at weak scale μ_W at LO in the MSSM with QFV.

Then we compute $C_7(\mu_b)$ and $C'_7(\mu_b)$ at

b-quark mass scale μ_b

by using RG QCD scale evolution at LL.

RG QCD scale evolution at LO:
$C_7(\mu_W) / C'_7(\mu_W) \rightarrow C_7(\mu_b) / C'_7(\mu_b)$
$(\mu_W = 160 \text{ GeV and } \mu_b = 4.8 \text{GeV})$

- $C_7(\mu_b) = \eta^{(16/23)} C_7(\mu_W) + (8/3)(\eta^{(14/23)} - \eta^{(16/23)}) C_8(\mu_W) + (\Sigma_{i=1-8} h_i \eta^{a_i})$

- $C'_7(\mu_b) = \eta^{(16/23)} C'_7(\mu_W) + (8/3)(\eta^{(14/23)} - \eta^{(16/23)}) C'_8(\mu_W)$
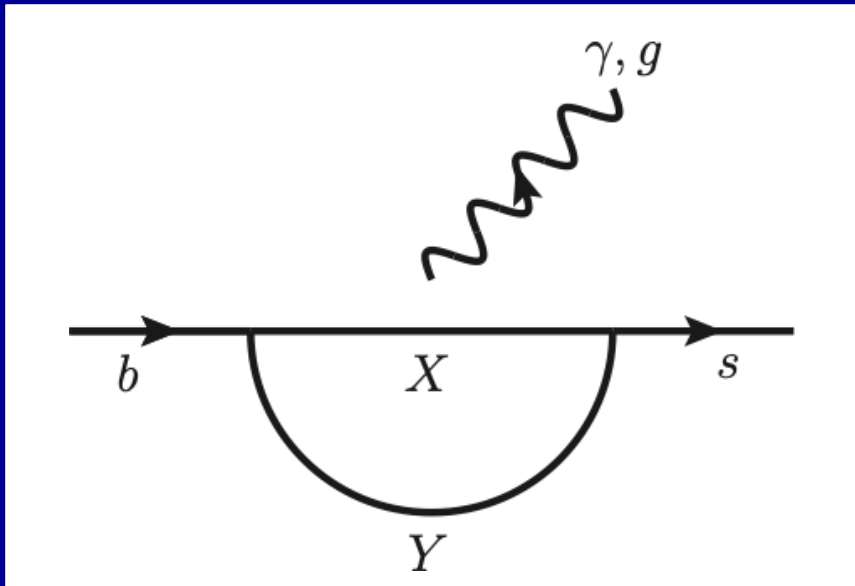
With

$\eta = \alpha_S(\mu_W)/\alpha_S(\mu_b)$

$h_i = (626126/272277, -56281/51730, -3/7, -1/14, -0.6494, -0.0380, -0.0186, -0.0057)$

$a_i = (14/23, 16/23, 6/23, -12/23, 0.4086, -0.4230, -0.8994, 0.1456)$

1-Loop contributions to $C_{7,8}(\mu_W)$ and $C'_{7,8}(\mu_W)$ at weak scale μ_W =160 GeV

SM one-loop contributions:
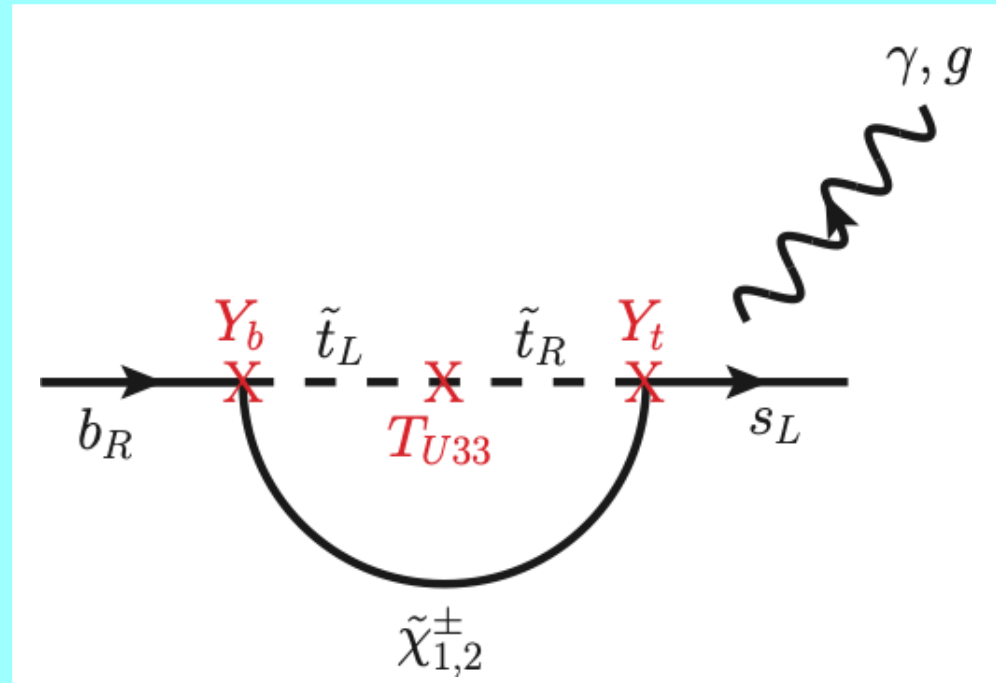$(X,Y) = (t/c/u, W^+)$

MSSM one-loop contributions:
$(X,Y) = (stop/scharm, chargino),$
$\qquad (sbottom/sstrange, gluino),$
$\qquad (sbottom/sstrange, neutralino),$
$\qquad (t/c/u, H^+)$

$\tilde{t}_L$ - $\tilde{t}_R$ loop contributions to $C_{7,8}(\mu_W)$:

$\tilde{\chi}^\pm \sim \tilde{W}^\pm + \tilde{H}^\pm$

Y_b : bottom Yukawa

Y_t : top Yukawa
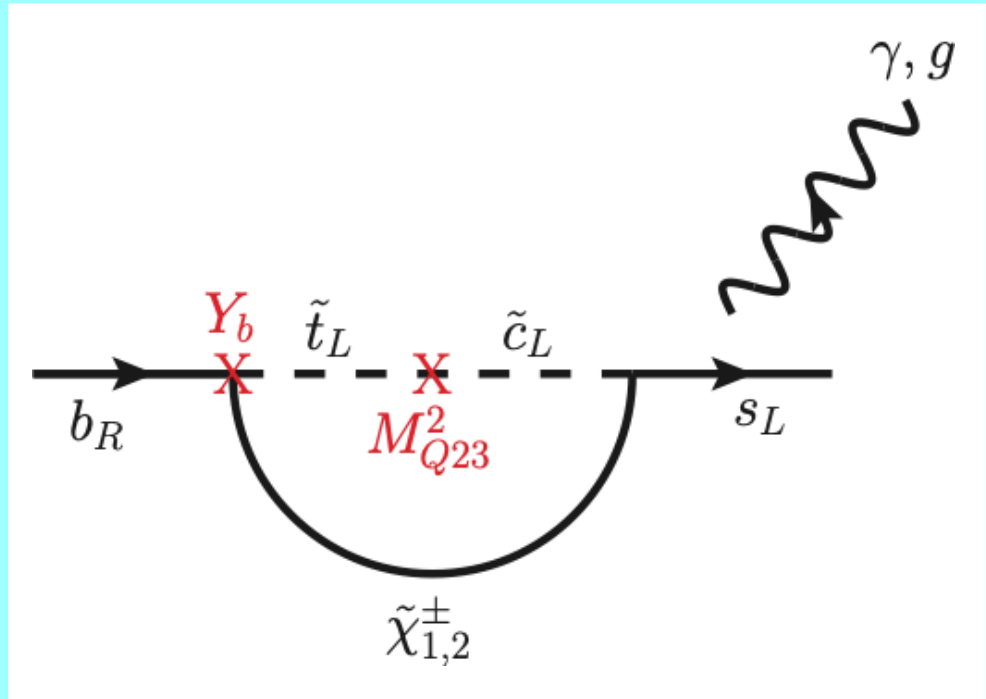

$\tilde{t}_L$ - $\tilde{t}_R$ loop contributions to $C_{7,8}(\mu_W)$ can be enhanced by large trilinear couplings T_{U33} and large Y_b for large $\tan\beta$ and large Y_t!

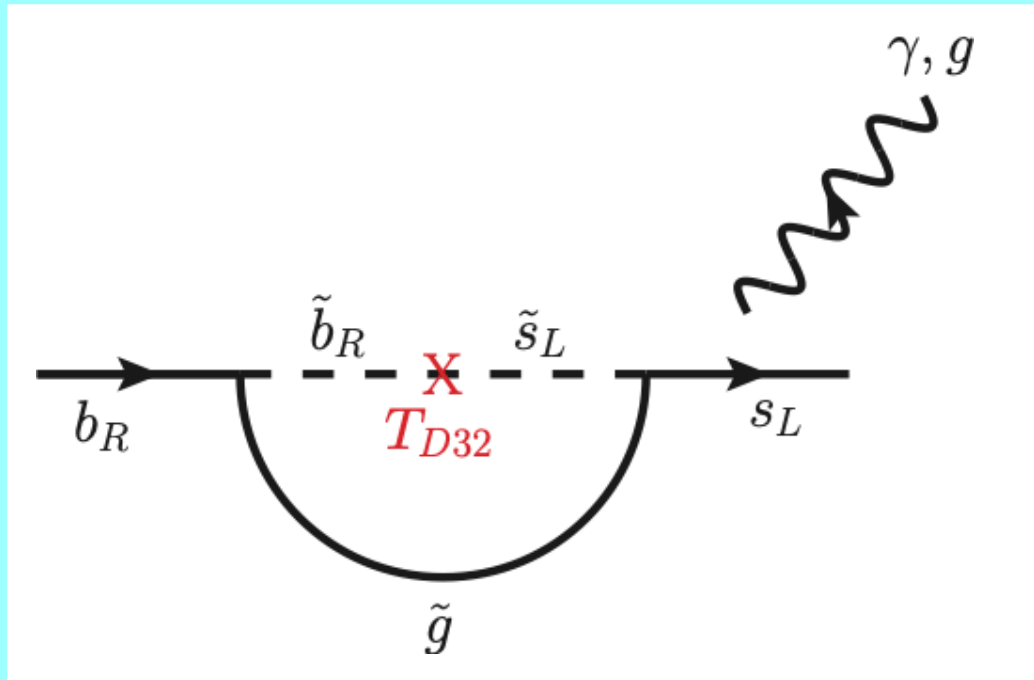**$\tilde{t}$ - $\tilde{c}$ loop contributions to $C_{7, 8}(\mu_W)$:**

$\tilde{\chi}^{\pm} \sim \tilde{W}^{\pm} + \tilde{H}^{\pm}$

Y_b : *bottom Yukawa*

$\tilde{t}$ - $\tilde{c}$ loop contributions to $C_{7, 8}(\mu_W)$ can be enhanced by large $\tilde{t}_L$ - $\tilde{c}_L$ mixing term M^2_{Q23} and large Y_b for large $\tan\beta$!

$\tilde{b}$ - $\tilde{s}$ loop contributions to $C_{7,8}(\mu_W)$:

$|T_{D32}|$ is controlled by Y_b due to vacuum stability condition.

$\tilde{b}$ - $\tilde{s}$ loop contributions to $C_{7,8}(\mu_W)$ can be enhanced by large trilinear coupling T_{D32} and large Y_b for large $\tan\beta$!

$\tilde{b}$ - $\tilde{s}$ loop contributions to $C'_{7,\,8}$ (μ_W):
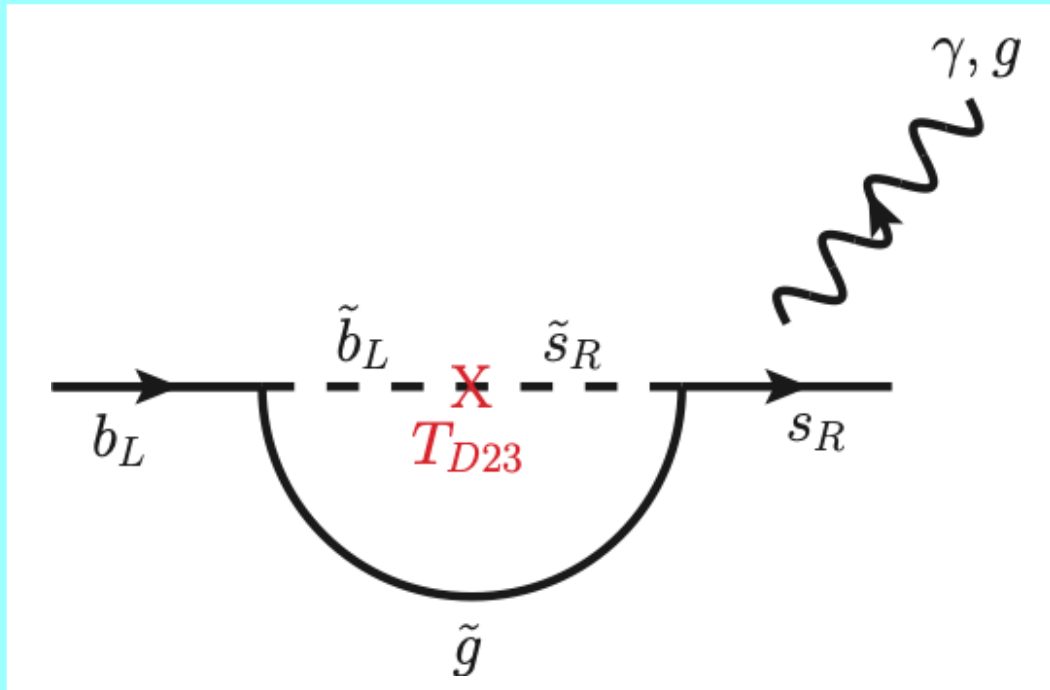

$|T_{D23}|$ is controlled by Y_b due to vacuum stability condition.

$\tilde{b}$ - $\tilde{s}$ loop contributions to $C'_{7,\,8}$ (μ_W) can be enhanced by large trilinear coupling T_{D23} and large Y_b for large $\tan\beta$!

Considering higher order MI contributions to the WCs $C_{7,8}$ & $C'_{7,8}$, MIs of $T_{U23,32}$, T_{D33}, M^2_{U23} and M^2_{D23} can also contribute to the WCs!

- *large trilinear couplings $T_{U23,32,33}$ & $T_{D23,32,33}$*
- *large QFV soft-mass-terms M^2_{Q23}, M^2_{U23}, M^2_{D23}*
- *large Y_b for large $\tan\beta$ and large Y_t*

Large MSSM one-loop contributions to $C_{7,8}(\mu_W)$ and $C'_{7,8}(\mu_W)$ at weak scale μ_W!

Large MSSM one-loop contributions to $C_7(\mu_b)$ and $C'_7(\mu_b)$ at b-quark mass scale μ_b!

Scatter Plot in ReC'$_7(\mu_b)$-ImC'$_7(\mu_b)$ plane
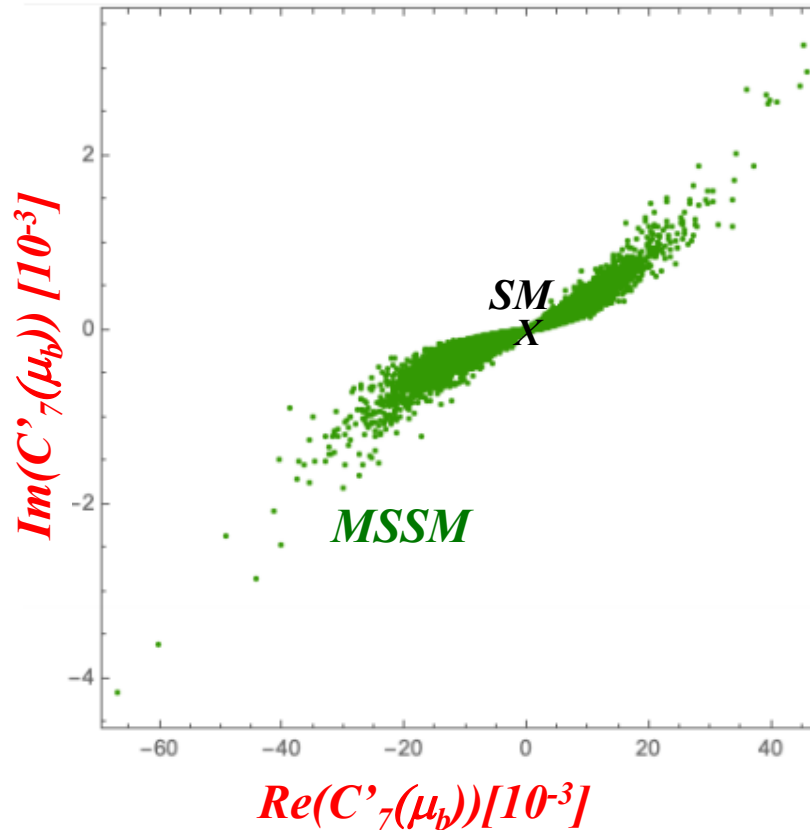
The MSSM contribution to Re(C'$_7(\mu_b)$) can be as large as ~ **-0.07** which could correspond to about **4σ New Physics (NP) signal significance** in future LHCb Upgrade and Belle II experiments.

Expected 1σ errors of ReC'₇(μ_b)-ImC'₇(μ_b) obtained from future LHCb Upgrade and Belle II
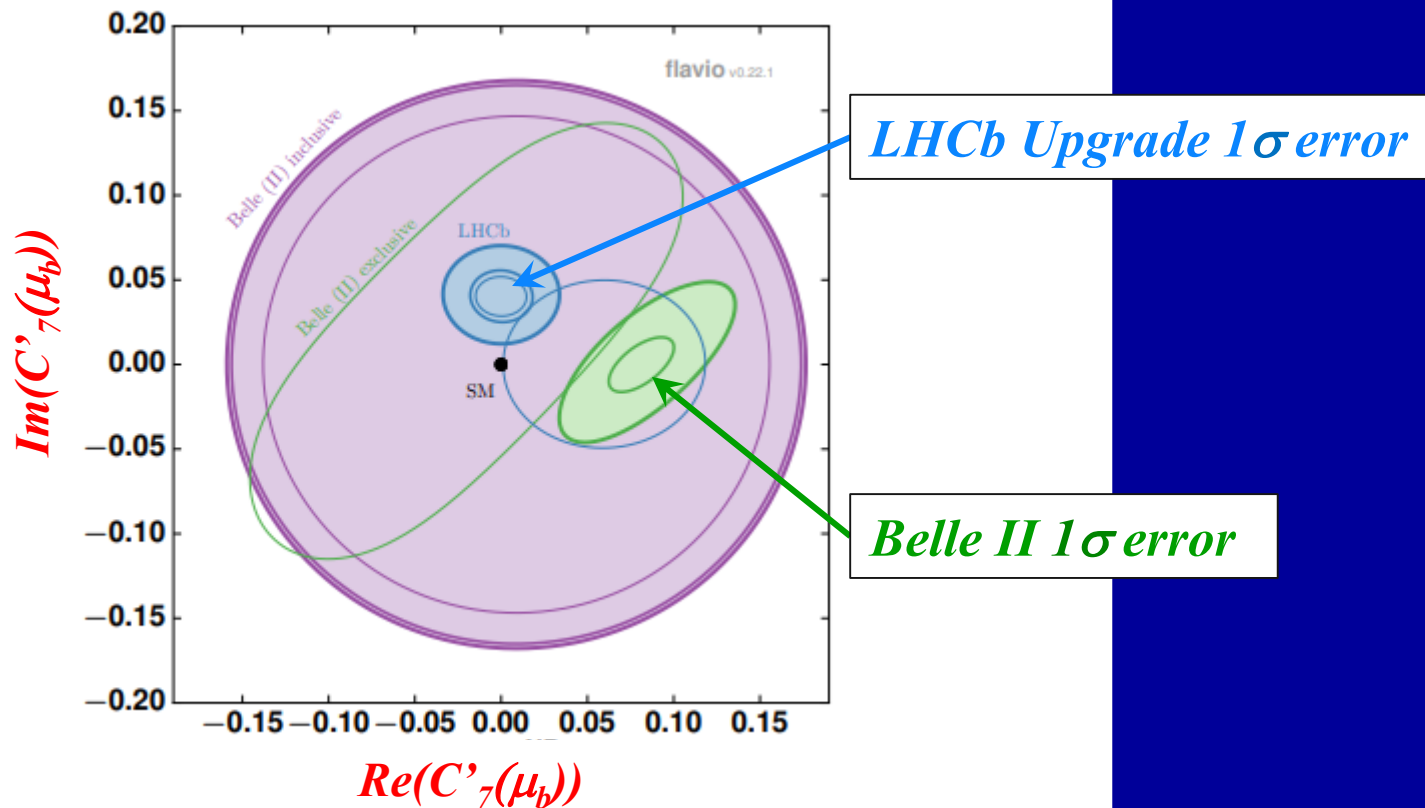
Belle II Physics Book, arXiv:1808.10567;
LHCb II Physics Book, arXiv:1808.08865;
Albrecht et al., arXiv:1709.10308.

Current Constraints at 2 sigma level in the $Re[C'_7(\mu_b)/C_7(\mu_b)]$-$Im[C'_7(\mu_b)/C_7(\mu_b)]$ plane

Constraints at 2σ
— $\mathcal{B}(B \to X_s\gamma)$
— $B^0 \to K_S^0\pi^0\gamma$
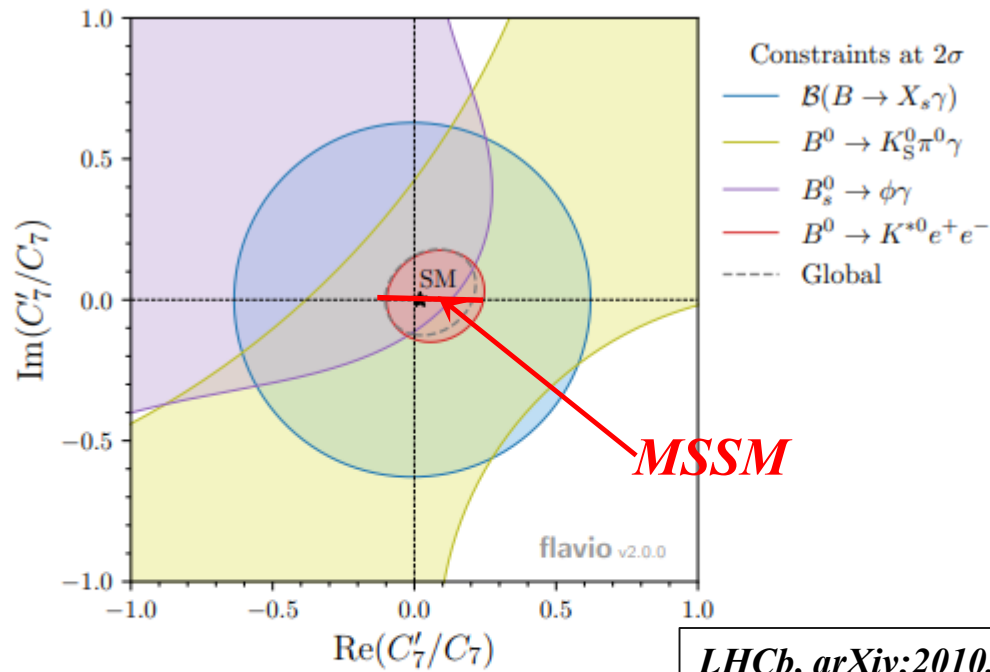— $B_s^0 \to \phi\gamma$
— $B^0 \to K^{*0}e^+e^-$
---- Global

MSSM

flavio v2.0.0

LHCb, arXiv:2010.06011

Figure 4: Constraints at 2σ level on the real and imaginary parts of the ratio of right- and left-handed Wilson coefficients, C'_7 and C_7. The C_7 coefficient is fixed to its SM value. The measurements of the inclusive branching fraction, $\mathcal{B}(B \to X_s\gamma)$, and the $B^0 \to K_S^0\pi^0\gamma$ mixing-induced CP asymmetry by the Belle and BaBar experiments [11–17] are shown in blue and yellow, respectively, the $B_s^0 \to \phi\gamma$ measurements at LHCb [18] in purple and the measurement presented in this paper in red. The global fit is shown in dashed lines and the SM prediction is represented by a black star and corresponds to the ratio of s- and b-quark masses.

Most of the MSSM points are still allowed by the current constraints including that from LHCb, arXiv:2010.06011!

Current Constraints at 2 sigma level in the Re[C'$_7$(μ_b)/C$_7$(μ_b)]-Im[C'$_7$(μ_b)/C$_7$(μ_b)] plane

LHCb, arXiv:2010.06011

Caveat:

flavio does not perform global fit!; i.e.
it perform a fit by taking just Re(C'$_7$) & Im(C'$_7$) as free parameters with all the other WCs fixed to their SM vakues!
If we perform a fit by taking all the relevant WCs as free parameters, then the allowed region in the Re(C'$_7$)-Im(C'$_7$) plane would become significantly larger!

Scatter Plot in ReC$_7^{MSSM}(\mu_b)$-ImC$_7^{MSSM}(\mu_b)$ plane
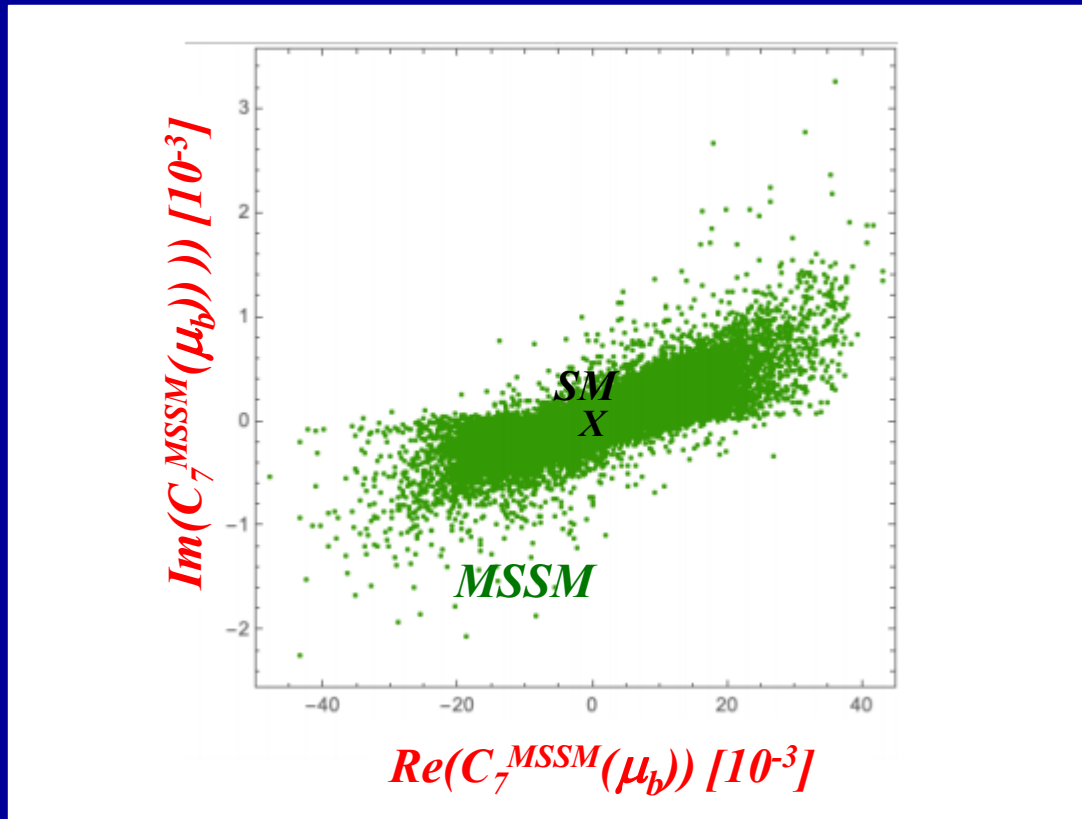
The MSSM contribution to Re(C$_7(\mu_b)$) can be as large as ~ -0.05 which could correspond to about 3σ NP signal significance in future LHCb and Belle II experiments.

Expected errors of $ReC_7^{NP}(\mu_b)$-$ImC_7^{NP}(\mu_b)$ obtained from future LHCb Upgrade and Belle II
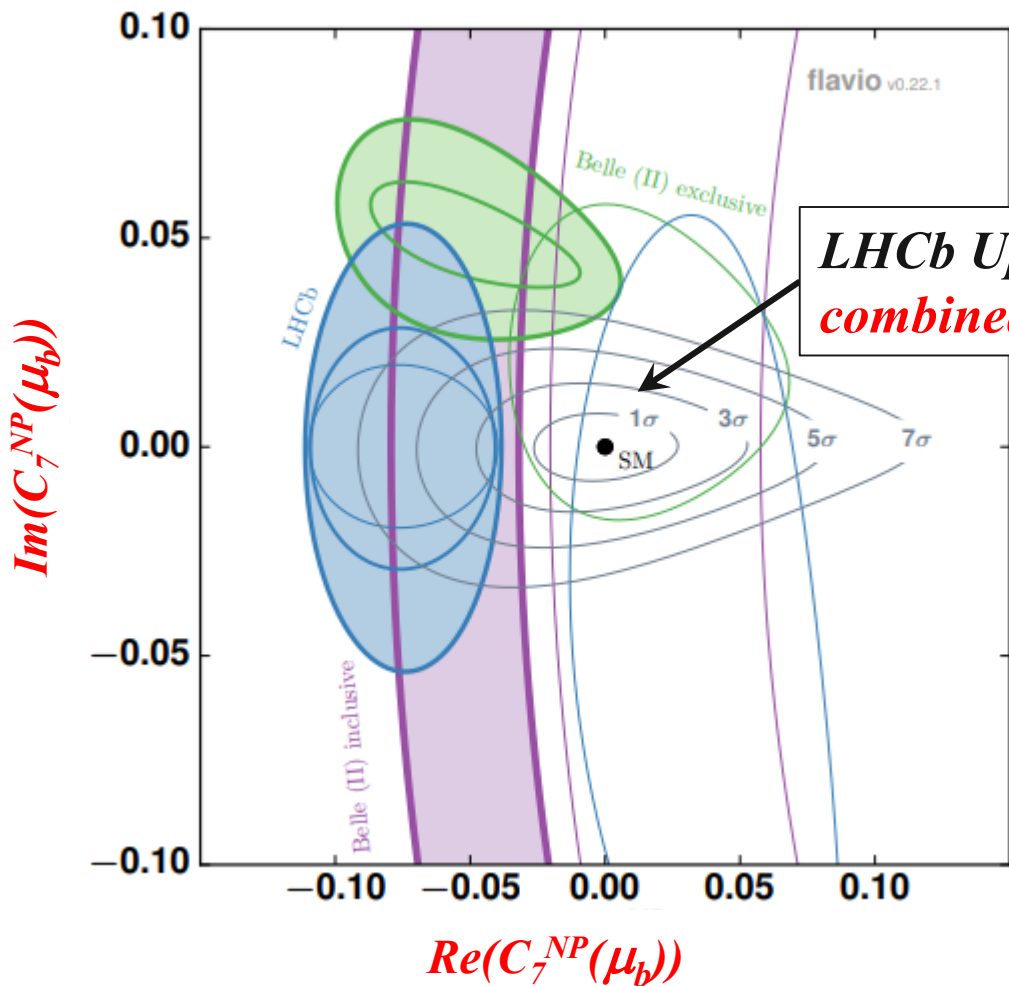
Belle II Physics Book, arXiv:1808.10567;
LHCb II Physics Book, arXiv:1808.08865;
Albrecht et al., arXiv:1709.10308.

Scatter Plot in $ReC_7^{MSSM}(\mu_b)$-$ReC'_7(\mu_b)$ plane
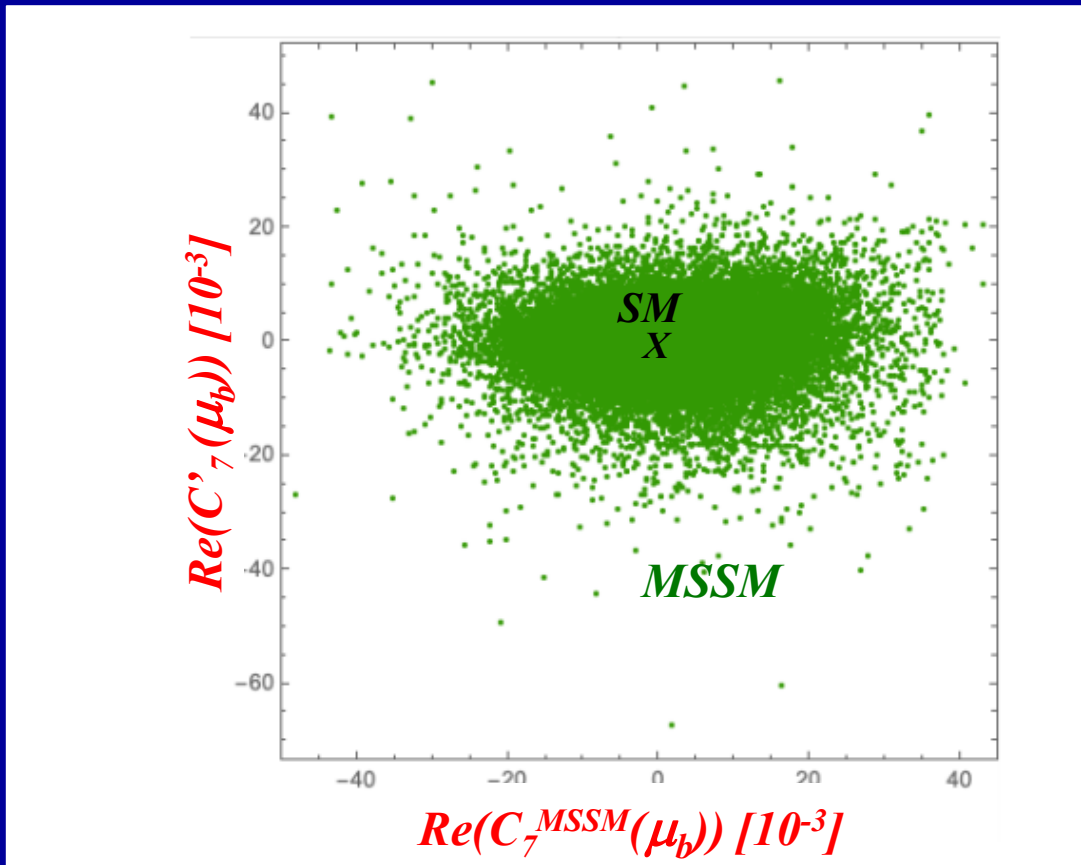
$Re(C_7^{MSSM}(\mu_b))$ and $Re(C'_7(\mu_b))$ can be quite sizable simultaneously!

Scatter plot in $T_{U23} - Re(C'_7(\mu_b))$ plane
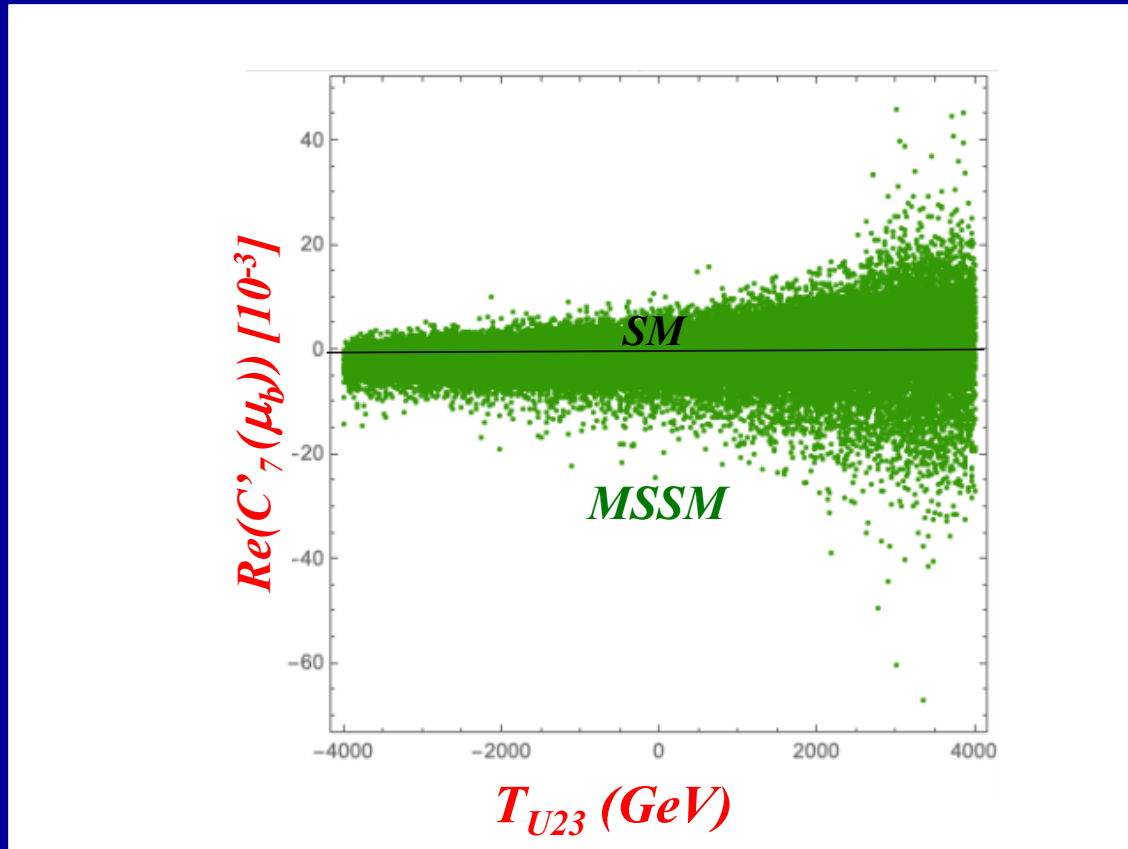
- *MSSM one-loop contributions to $Re(C'_7(\mu_b))$ can be large (-0.07 ~ +0.05) for large T_{U23} (> 0)!*
- *$Re(C'_7(\mu_b)) \approx 0$ (SM)*

- *MSSM one-loop contributions to Re(C'$_7$(μ$_b$)) can be large (-0.07 ~ +0.05) for large tanβ (> 40)!*
- *This behavior is consistent with our expectation!*

Scatter plot in $T_{U23} - Re(C_7^{MSSM}(\mu_b))$ plane
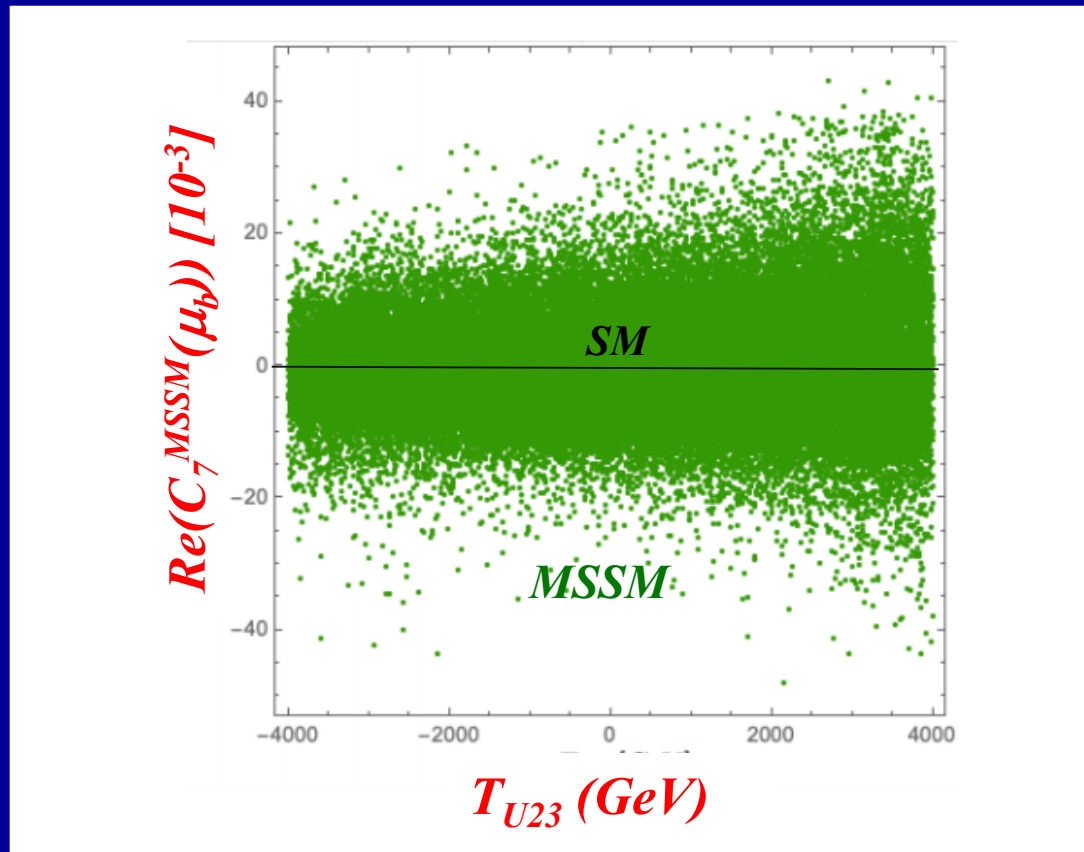
- **MSSM one-loop contributions to $Re(C_7(\mu_b))$ can be large ($\sim \pm 0.05$) for large T_{U23} (> 0)!**

Scatter plot in $\tan\beta - Re(C_7^{MSSM}(\mu_b))$ plane
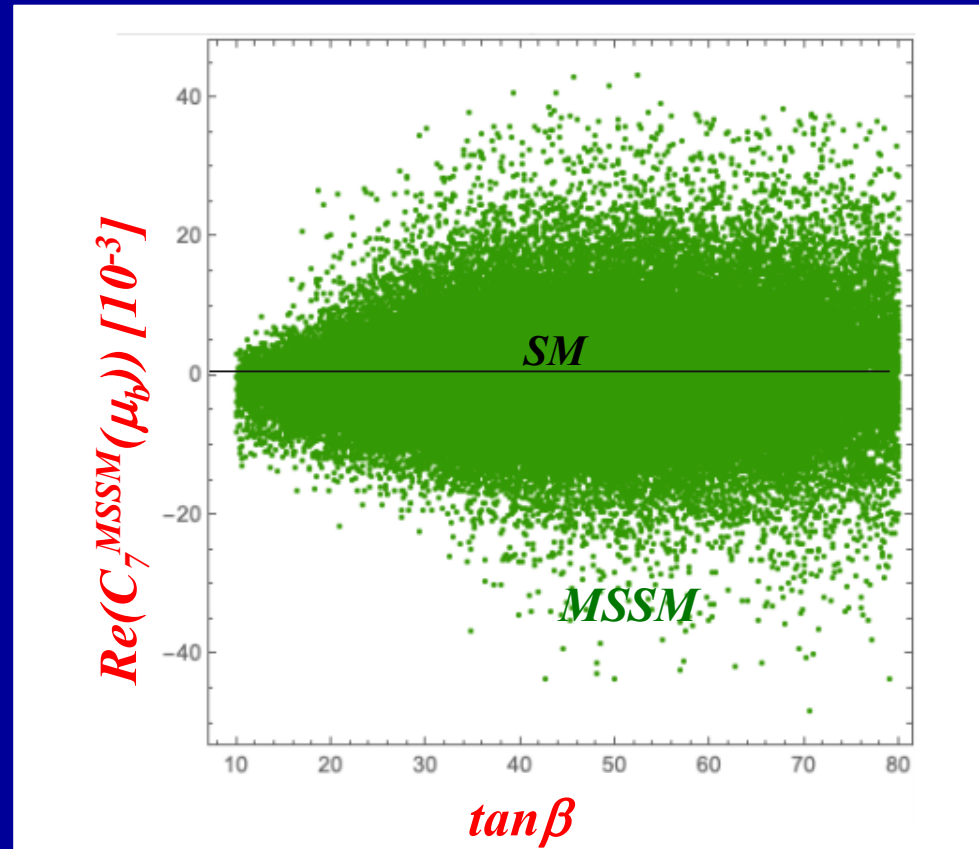
- *MSSM one-loop contributions to $Re(C_7(\mu_b))$ can be large ($\sim \pm 0.05$) for large $\tan\beta$ (> 40)!*
- *This behavior is consistent with our expectation!*

6. Conclusion

- *We have studied **SUSY effects on $C_7(\mu_b)$ and $C'_7(\mu_b)$** which are the Wilson coefficients for b -> s gamma at b-quark mass scale μ_b and are closely related to radiative B meson decays.*

- *The SUSY-loop contributions to the $C_7(\mu_b)$ and $C'_7(\mu_b)$ are calculated in the **MSSM with general quark flavor violation (QFV)** and real parameters at LO.*

- *In the computation of the WCs, **for the first time**, we have performed a **systematic MSSM parameter scan** respecting all the relevant constraints, i.e. theoretical constraints from vacuum stability conditions and experimental constraints, such as those from K- & B-meson data and electroweak precision data, as well as recent limits on SUSY particle masses and H(125) data from LHC experiments.*

- *From the parameter scan, we have found the following:*

  (1) The MSSM contribution to Re($C_7(\mu_b)$) can be as large as ~ ± 0.05
  which could correspond to about 3σ New Physics (NP) signal significance
  in future LHCb Upgrade and Belle II experiments.

  (2) The MSSM contribution to Re($C'_7(\mu_b)$) can be as large as ~ -0.08
  which could correspond to about 4σ NP signal significance
  in future LHCb Upgrade and Belle II experiments.

  (3) These large MSSM contributions to the WC's are mainly due to
  - large $\tilde{c}$ - $\tilde{t}$ mixing & large $\tilde{c}/\tilde{t}$ trilinear couplings T_{U23}, T_{U32}, T_{U33},
  - large $\tilde{s}$ - $\tilde{b}$ mixing & large $\tilde{s}/\tilde{b}$ trilinear couplings T_{D23}, T_{D32}, T_{D33},
  - large Y_b for large tanβ and large Y_t.

- *In case such large New Physics contributions to the WCs are really observed in
  the future experiments at Belle II and LHCb Upgrade, it could be the imprint of
  QFV SUSY (MSSM with QFV) and would encourage to perform further studies
  of the WCs at NLO/NNLO level in this model .*

- *Our analysis suggests the following:*

PETRA/TRISTAN e- e+ collider discovered virtual Z^0 effect for the first time.

Later, CERN p $\bar{p}$ collider discovered the Z^0 boson.

Similarly, Belle II / LHCb Upgrade could discover virtual Sparticle effects for the first time in radiative

B meson decays!

Later, FCC-hh p p collider could discover the Sparticles!

END

Thank you!

Backup Slides

2. <u>*MSSM with QFV*</u>

The basic parameters of the MSSM with QFV:

$$\{tan\beta, m_A, M_1, M_2, M_3, \mu, M^2_{Q,\alpha\beta}, M^2_{U,\alpha\beta}, M^2_{D,\alpha\beta}, T_{U\alpha\beta}, T_{D\alpha\beta}\}$$

(at Q = 1 TeV scale)   *(α,β = 1,2,3 = u, c, t or d, s, b)*

$tan\beta$:   *ratio of VEV of the two Higgs doublets* $<H^0_2>/<H^0_1>$

m_A :   *CP odd Higgs boson mass (pole mass)*

M_1, M_2, M_3 :   *U(1), SU(2),SU(3) gaugino masses*

μ :   *higgsino mass parameter*

$M^2_{Q,\alpha\beta}$: *left squark soft mass matrix*

$M^2_{U\alpha\beta}$:   *right up-type squark soft mass matrix*

$M^2_{D\alpha\beta}$:   *right down-type squark soft mass matrix*

$T_{U\alpha\beta}$:   *trilinear coupling matrix of up-type squark and Higgs boson*

$T_{D\alpha\beta}$:   *trilinear coupling matrix of down-type squark and Higgs boson*

We work in the MSSM with real parameters, except for the CKM matrix.

Constraints on the MSSM parameters from K & B meson and h^0 data:

Table 5: Constraints on the MSSM parameters from the K- and B-meson data relevant mainly for the mixing between the second and the third generations of squarks and from the data on the h^0 mass and couplings κ_b, κ_g, κ_γ. The fourth column shows constraints at 95% CL obtained by combining the experimental error quadratically with the theoretical uncertainty, except for $B(K_L^0 \to \pi^0 \nu \bar\nu)$, m_{h^0} and $\kappa_{b,g,\gamma}$.

Observable	Exp. data	Theor. uncertainty	Constr. (95%CL)
$10^3 \times \lvert\epsilon_K\rvert$	2.228 ± 0.011 (68% CL) [21]	± 0.28 (68% CL) [40]	2.228 ± 0.549
$10^{15} \times \Delta M_K$ [GeV]	3.484 ± 0.006 (68% CL) [21]	± 1.2 (68% CL) [40]	3.484 ± 2.352
$10^9 \times B(K_L^0 \to \pi^0 \nu\bar\nu)$	< 3.0 (90% CL) [21]	± 0.002 (68% CL) [21]	< 3.0 (90% CL)
$10^{10} \times B(K^+ \to \pi^+ \nu\bar\nu)$	1.7 ± 1.1 (68% CL) [21]	± 0.04 (68% CL) [21]	$1.7^{+2.16}_{-1.70}$
ΔM_{B_s} [ps^{-1}]	17.757 ± 0.021 (68% CL) [21,41]	± 2.7 (68% CL) [42]	17.757 ± 5.29
$10^4 \times B(b \to s\gamma)$	3.32 ± 0.15 (68% CL) [21,41]	± 0.23 (68% CL) [11]	3.32 ± 0.54
$10^6 \times B(b \to s\, l^+l^-)$	$1.60^{+0.48}_{-0.45}$ (68% CL) [43]	± 0.11 (68% CL) [44]	$1.60^{+0.97}_{-0.91}$
($l = e$ or μ)			
$10^9 \times B(B_s \to \mu^+\mu^-)$	$2.69^{+0.37}_{-0.35}$ (68%CL) [45]	± 0.23 (68% CL) [46]	$2.69^{+0.85}_{-0.82}$
$10^4 \times B(B^+ \to \tau^+\nu)$	1.06 ± 0.19 (68%CL) [41]	± 0.29 (68% CL) [47]	1.06 ± 0.69
m_{h^0} [GeV]	125.09 ± 0.24 (68% CL) [48]	± 3 [49]	125.09 ± 3.48
κ_b	$1.06^{+0.37}_{-0.35}$ (95% CL) [50]		$1.06^{+0.37}_{-0.35}$ (ATLAS)
	$1.17^{+0.53}_{-0.61}$ (95% CL) [51]		$1.17^{+0.53}_{-0.61}$ (CMS)
κ_g	$1.03^{+0.14}_{-0.12}$ (95% CL) [50]		$1.03^{+0.14}_{-0.12}$ (ATLAS)
	$1.18^{+0.31}_{-0.27}$ (95% CL) [51]		$1.18^{+0.31}_{-0.27}$ (CMS)
κ_γ	1.00 ± 0.12 (95% CL) [50]		1.00 ± 0.12 (ATLAS)
	$1.07^{+0.27}_{-0.29}$ (95% CL) [51]		$1.07^{+0.27}_{-0.29}$ (CMS)

Constraints on the MSSM parameters from W boson mass data:

The recent m_W data from CDF II [1] is quite inconsistent with the other experimental data. (-> See next slides.)
 [1] *CDF Collaboration, Science 376, 170–176 (2022)*

This issue of the m_W data is not yet settled.

Hence, we do not take into accont this m_W constraint on the MSSM parameters in our analysis.

What to think of m_W measurements?
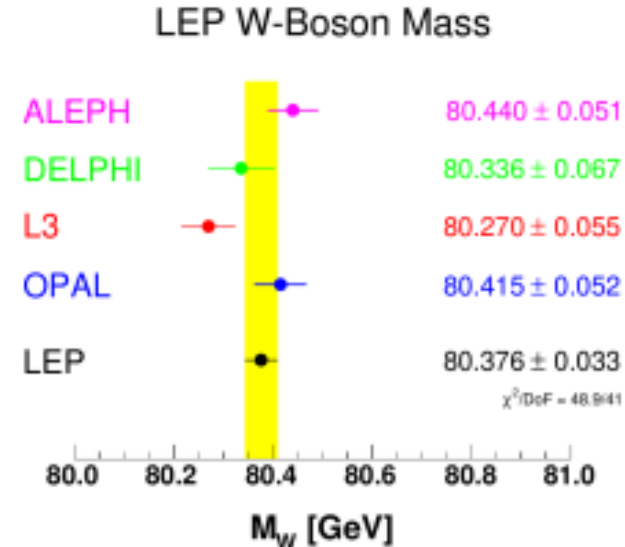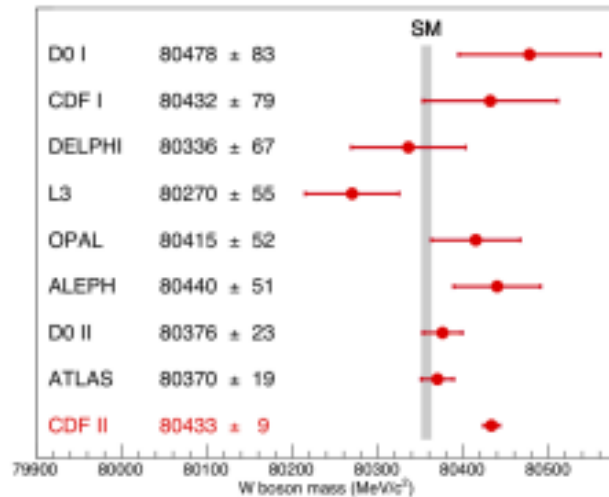
- The LEP results are based on 42 separate measurements with a **healthy** χ^2.
- The LEP-combined (33 MeV), LHCb (32 MeV), D0 Run II (23 MeV), ATLAS (19 MeV) and CDF Run II (9.4 MeV) measurements have a $\chi^2/$DoF $= 17.1/4$, with p-value of **0.2%** for compatibility (neglecting correlations).
- So reasonably strong evidence that the ensemble of experimental results are **inconsistent with each other** independent of any SM prediction.
- The standard PDG procedure is to add a scale factor "democratically" to all measurements to parametrize our ignorance.

PDG scale factors

(What can happen with supposed high precision measurements)
The new world average m_W uncertainty should be scaled up by about 2.1 leading to an uncertainty of 15 MeV in PDG-2022 compared with 12 MeV in PDG-2020.

WEIGHTED AVERAGE
493.677±0.013 (Error scaled by 2.4)

Values above of weighted average, error, and scale factor are based upon the data in this idogram only. They are not necessarily the same as our 'best' values, obtained from a least-squares constrained fit utilizing measurements of other (related) quantities as additional information.

			χ^2
DENISOV	91	CNTR	7.7
GALL	88	CNTR	13.6
LUM	81	CNTR	
BARKOV	79	EMUL	0.1
CHENG	75	CNTR	1.0
BACKENBTO...73		CNTR	0.1
			22.4

(Confidence Level = 0.0002)

$m_{K^\pm}$ (MeV)

The charged kaon mass has been in this scale-factored state for 30 years!

Plot from Resonaances blog (Adam Falkowski). Independently I had also done this and concluded that the scale-factored world-average is $+3.2\sigma$ off the SM value used by CDF

Perhaps one or more experiments has underestimated uncertainties. Also may be difficult to measure the same thing in $p\bar{p}$, pp, and e^+e^- collisions.
Strong motivation to measure m_W well in complementary ways in e^+e^- collisions!

1. Introduction: the mass of the W-boson

[CDF '22]

D0 I	80478 ± 83	
CDF I	80432 ± 79	
DELPHI	80336 ± 67	
L3	80270 ± 55	
OPAL	80415 ± 52	
ALEPH	80440 ± 51	
D0 II	80376 ± 23	
ATLAS	80370 ± 19	
CDF II	80433 ± 9	

SM

W boson mass (MeV/c^2)
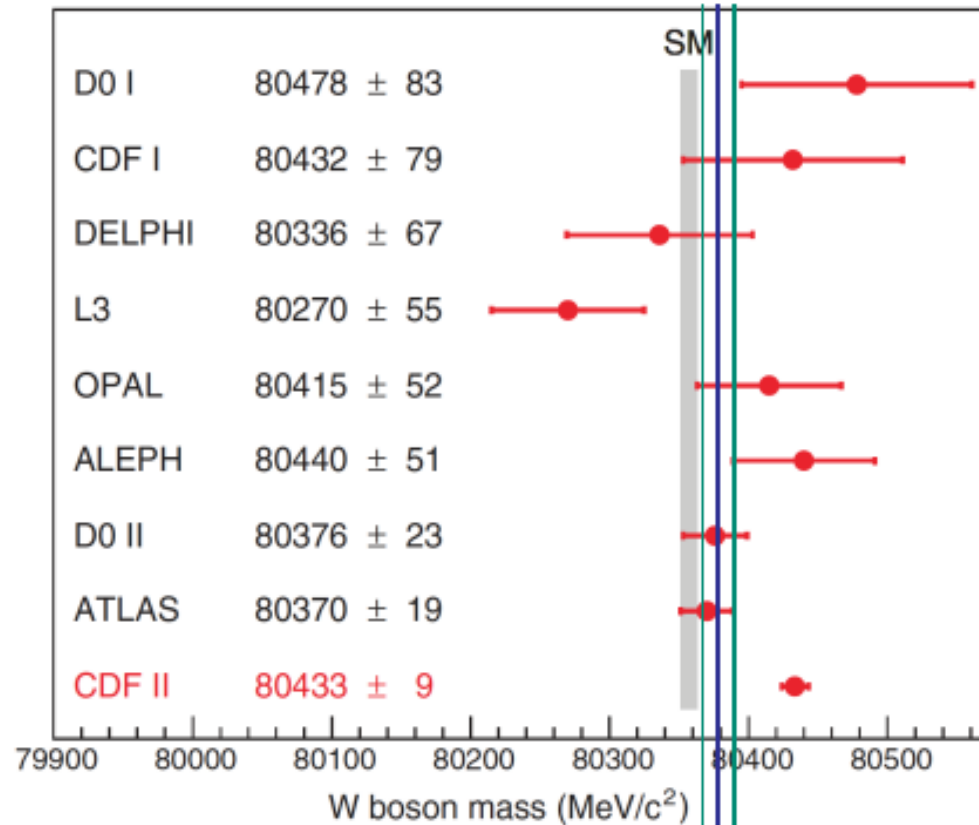
⇒ large discrepancy with the SM prediction

⇒ large discrepancy with other measurements: $M_W^{\mathrm{PDG}} = 80379 \pm 12$ MeV

Approximation for a new world average:

m_W [GeV]
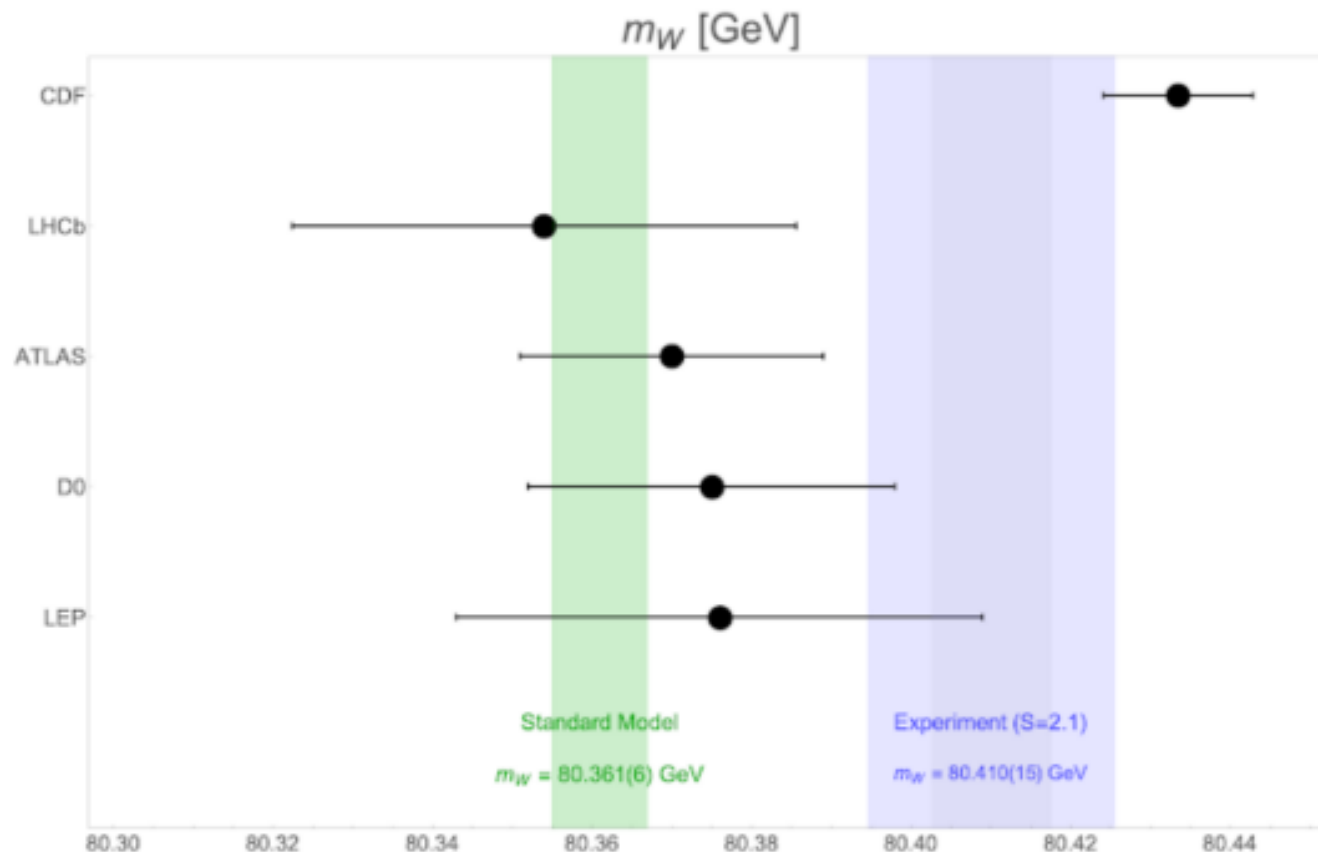
⇒ approximation yields $M_W^{\text{approx-av.}} = 80410 \pm 15$ MeV $\sim 3\sigma$

⇒ enlarged uncertainty because of "bad agreement" between older and new measurements ⇒ PDG prescription

4. *Parameter scan in the MSSM*

Table 1: Scanned ranges and fixed values of the MSSM parameters (in units of GeV or GeV^2, except for $\tan\beta$). The parameters that are not shown explicitly are taken to be zero. $M_{1,2,3}$ are the U(1), SU(2), SU(3) gaugino mass parameters.

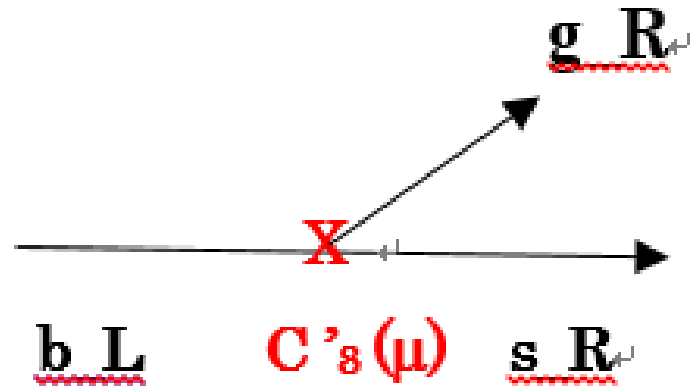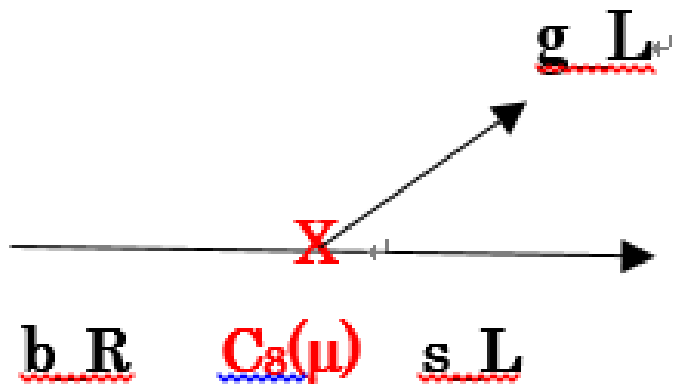| $\tan\beta$	M_1	M_2	M_3	μ	$m_A(pole)$
$10 \div 80$	$100 \div 2500$	$100 \div 2500$	$2500 \div 5000$	$100 \div 2500$	$1350 \div 6000$

M^2_{Q22}	M^2_{Q33}	$\lvert M^2_{Q23}\rvert$	M^2_{U22}	M^2_{U33}	$\lvert M^2_{U23}\rvert$
$2500^2 \div 4000^2$	$2500^2 \div 4000^2$	$< 1000^2$	$1000^2 \div 4000^2$	$600^2 \div 3000^2$	$< 2000^2$

M^2_{D22}	M^2_{D33}	$\lvert M^2_{D23}\rvert$	$\lvert T_{U23}\rvert$	$\lvert T_{U32}\rvert$	$\lvert T_{U33}\rvert$
$2500^2 \div 4000^2$	$1000^2 \div 3000^2$	$< 2000^2$	< 4000	< 4000	< 5000

$\lvert T_{D23}\rvert$	$\lvert T_{D32}\rvert$	$\lvert T_{D33}\rvert$	$\lvert T_{E33}\rvert$
< 3000	< 3000	< 4000	< 500

M^2_{Q11}	M^2_{U11}	M^2_{D11}	M^2_{L11}	M^2_{L22}	M^2_{L33}	M^2_{E11}	M^2_{E22}	M^2_{E33}
4500^2	4500^2	4500^2	1500^2	1500^2	1500^2	1500^2	1500^2	1500^2

γ_L

b_R $C_7(\mu)$ s_L

γ_R

b_L $C'_7(\mu)$ s_R

g_L

b_R $C_8(\mu)$ s_L

g_R

b_L $C'_8(\mu)$ s_R

$t - H^+$ loop contributions to $C_{7,8}(\mu_W)$:

γ, g

Y_b t_L t_R Y_t

b_R m_t s_L

H^+

$Y_{b,t}$: bottom, top Yukawa coupling

$t - H^+$ loop contributions to $C_{7,8}(\mu_W)$ can be enhanced by large Y_b for large $\tan\beta$ and large Y_t !
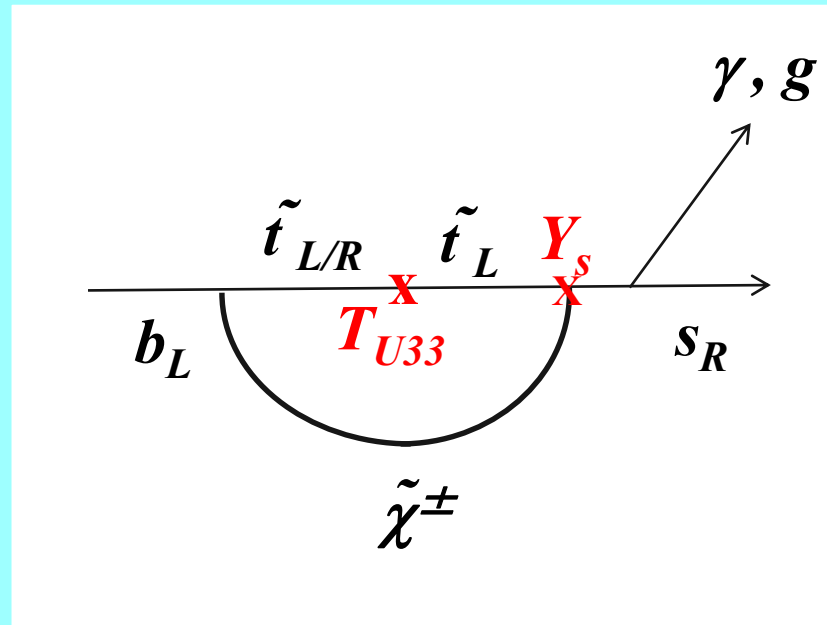
$\tilde{t}$ - $\tilde{t}$ loop contributions to C'$_{7, 8}$ (μ_W):

$\tilde{\chi}^{\pm} \sim \tilde{W}^{\pm} + \tilde{H}^{\pm}$

$\tilde{t}$ - $\tilde{t}$ loop contributions to C'$_{7, 8}$(μ_W) should be small due to very small Y_s!

$\tilde{t}$ - $\tilde{c}$ loop contributions to $C'_{7,8}(\mu_W)$:
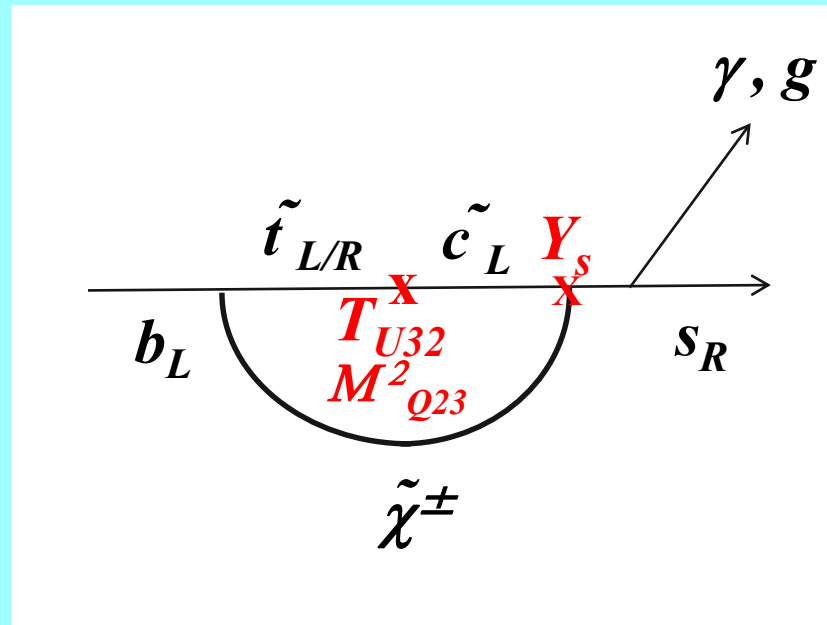
$$\tilde{\chi}^{\pm} \sim \tilde{W}^{\pm} + \tilde{H}^{\pm}$$

$\tilde{t}$ - $\tilde{c}$ loop contributions to $C'_{7,8}(\mu_W)$ should be small due to very small Y_s!
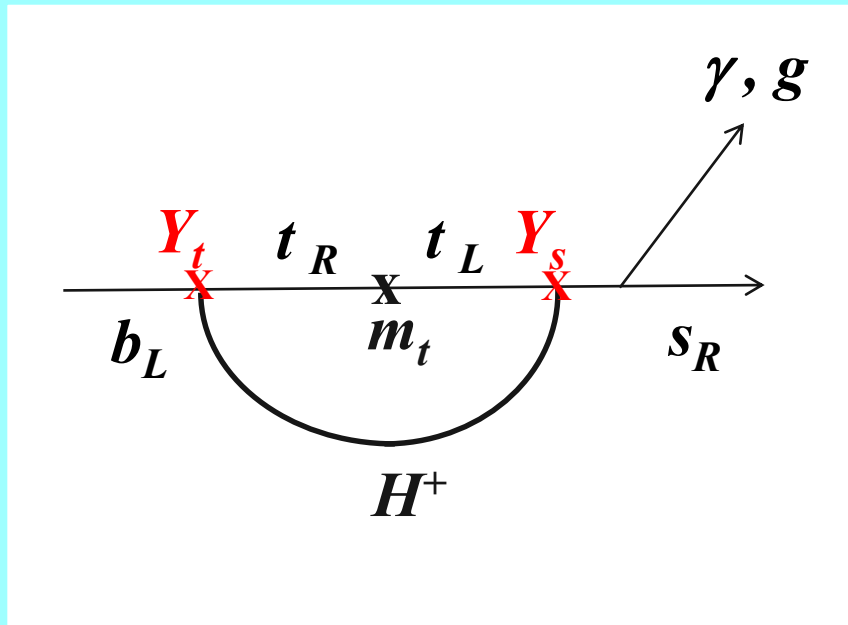
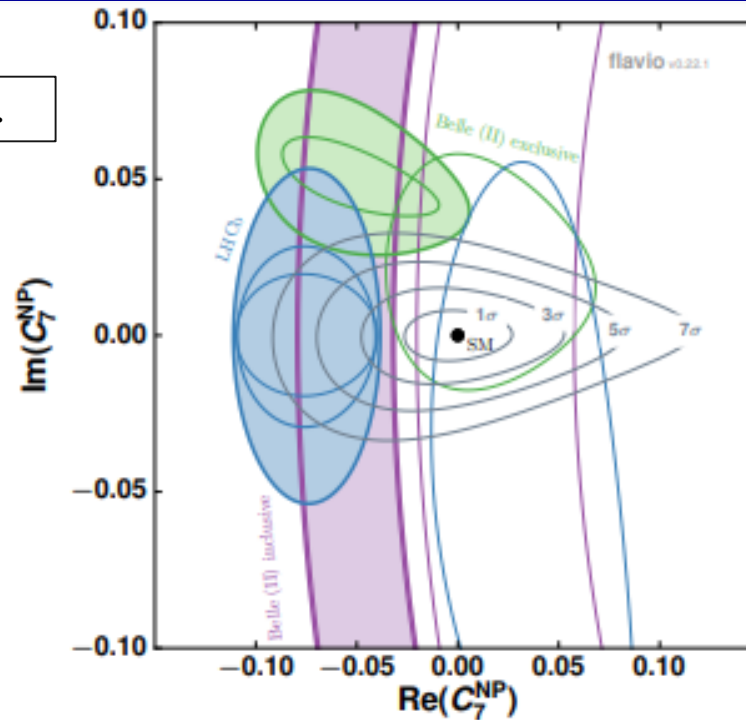**$t - H^+$ loop contributions to $C'_{7,8}(\mu_W)$:**

Y_t : top Yukawa coupling

Y_s : s quark Yukawa coupling

$t - H^+$ loop contributions to $C'_{7,8}(\mu_W)$ is small due to small Y_s.

Albrecht et al., arXiv:1709.10308.

(c) $\mathcal{Re}\left(C_7^{\mathrm{NP}}\right)$ versus $\mathcal{Im}\left(C_7^{\mathrm{NP}}\right)$.

Figure 8: In the two-dimensional scans of pairs of Wilson coefficients, the current average (not filled) as well as the extrapolations to future sensitivities (filled) of LHCb at milestones I, II and III (exclusive) and Belle II at milestones I and II (inclusive and exclusive) are given. The central values of the extrapolations have been evaluated in the NP scenarios listed in Table 5. The contours correspond to 1σ uncertainty bands. The Standard Model point (black dot) with the $1\sigma, 3\sigma, 5\sigma$ and 7σ exclusion contours with a combined sensitivity of LHCb's $50\,\mathrm{fb}^{-1}$ and Belle II's $50\,\mathrm{ab}^{-1}$ datasets is indicated in light grey. The primed operators show no tensions with respect to the SM; hence no SM exclusions are provided.

Scatter plot in $T_{D23} - Re(C'_7(\mu_b))$ plane
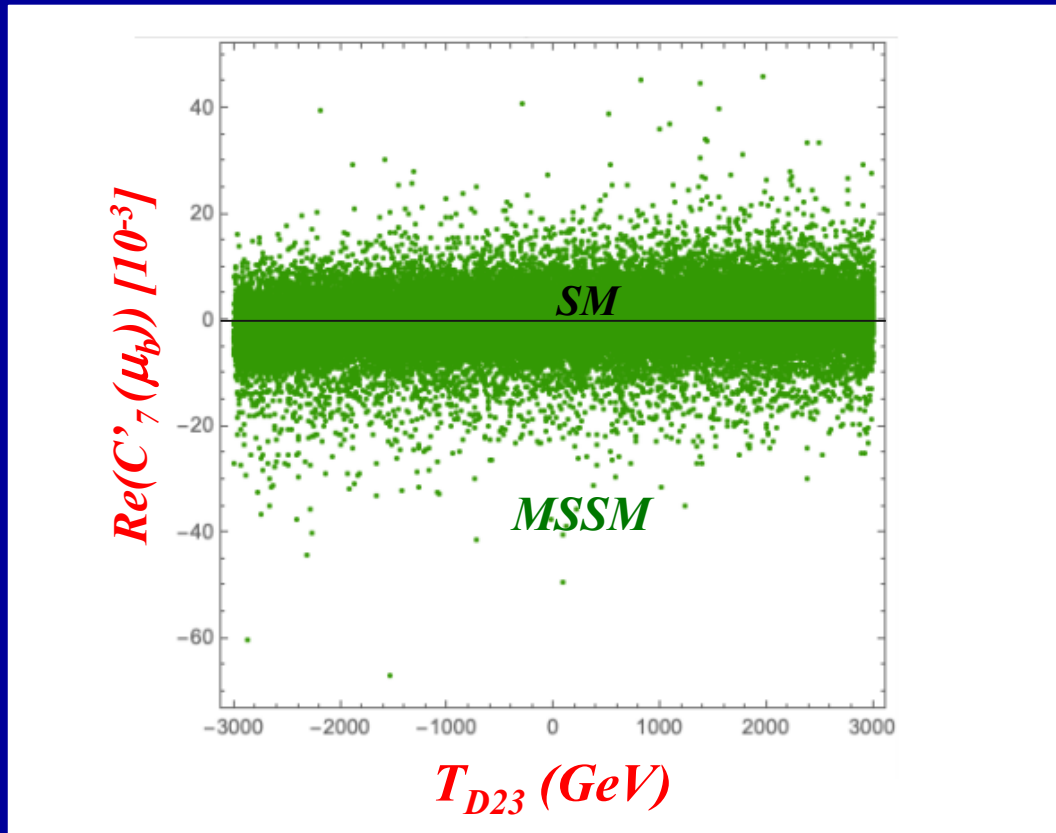
- *MSSM one-loop contributions to $Re(C'_7(\mu_b))$ can be large ($-0.07 \sim +0.05$) for large $|T_{D23}|$!*
- *There is an appreciable correlation between T_{D23} and $Re(C'_7(\mu_b))$!*

Scatter plot in $T_{D23} - Re(C_7^{MSSM}(\mu_b))$ plane

SM

MSSM

$Re(C_7^{MSSM}(\mu_b))$ $[10^{-3}]$

T_{D23} (GeV)
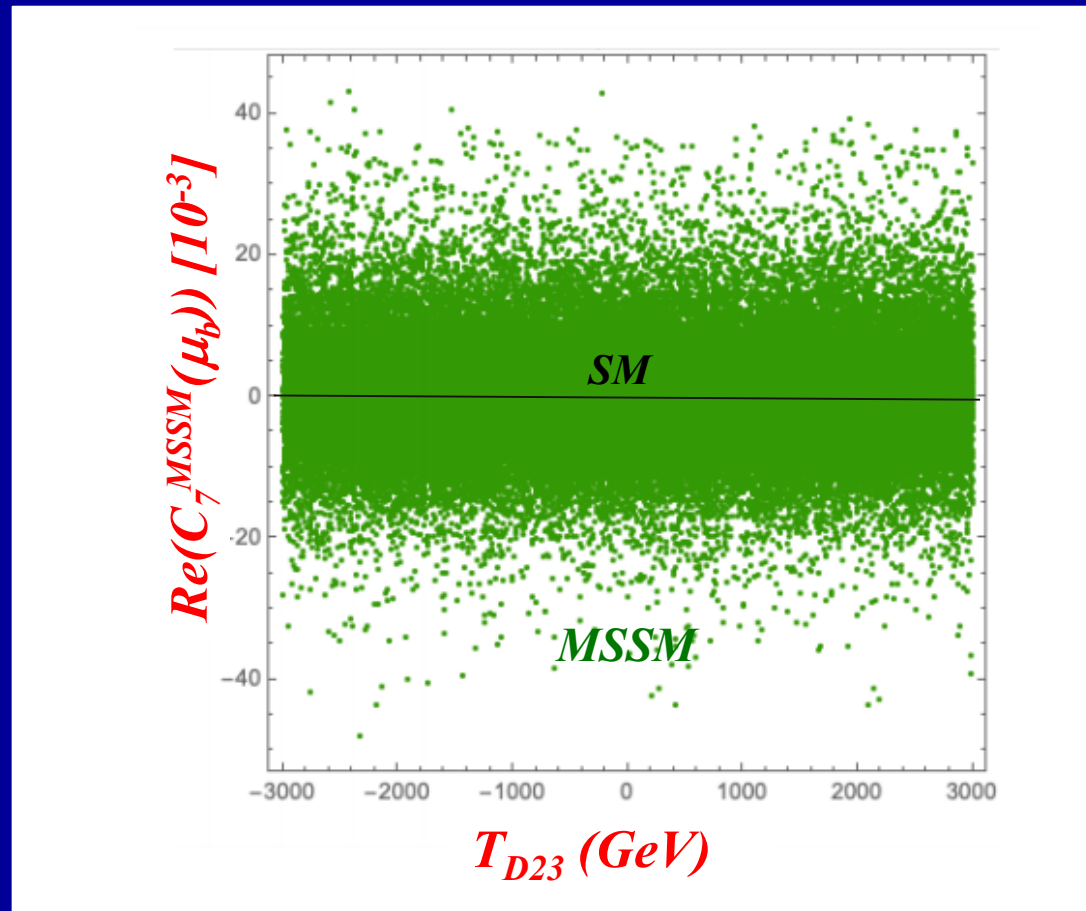
- MSSM one-loop contributions to $Re(C_7(\mu_b))$ can be large (~ ±0.05) for any value of T_{D23} !

Scatter plot in $T_{U33} - Re(C_7^{MSSM}(\mu_b))$ plane
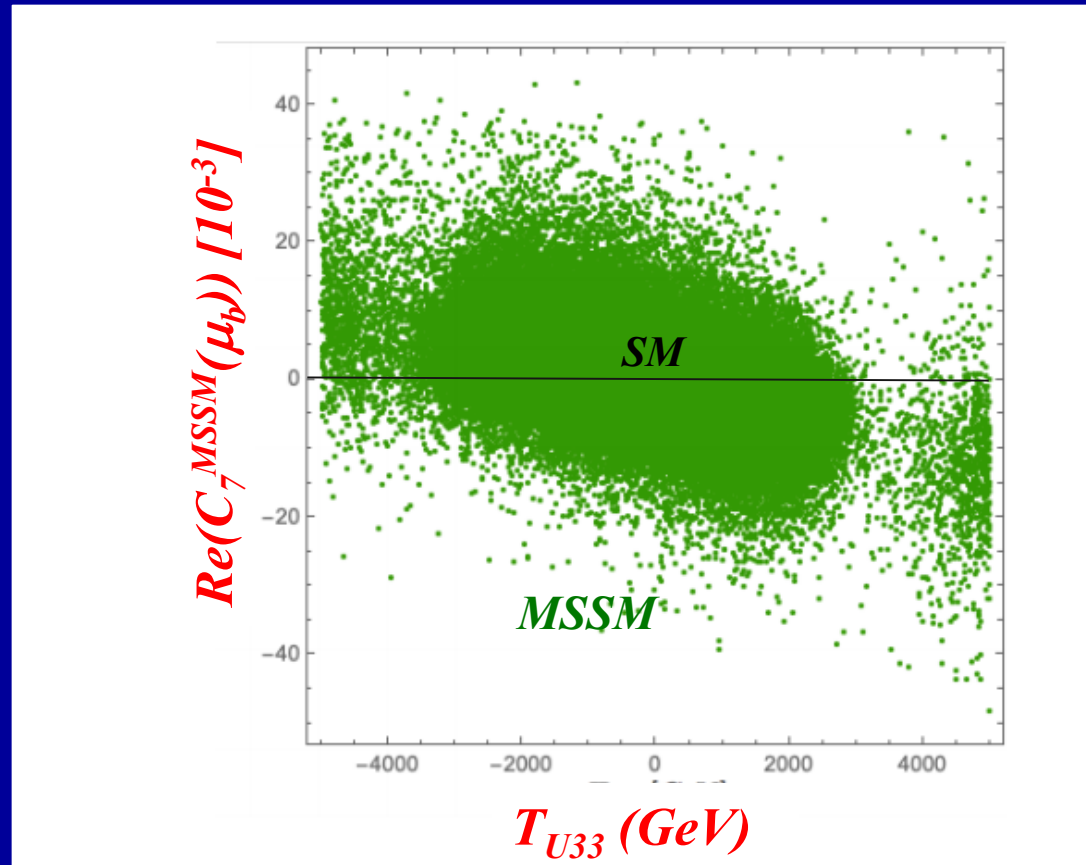
- *MSSM one-loop contributions to $Re(C_7(\mu_b))$ can be large (~ ±0.05) for large T_{U33}!*
- *There is a significant correlation between T_{U33} and $Re(C_7^{MSSM}(\mu_b))$!*

$\tilde{t}_L$ - $\tilde{t}_R$ loop contributions to $C_{7,\,8}(\mu_W)$:

$\tilde{\chi}^\pm \sim \tilde{W}^\pm + \tilde{H}^\pm$

Y_b : bottom Yukawa

Y_t : top Yukawa

$\tilde{t}_L$ - $\tilde{t}_R$ loop contributions to $C_{7,\,8}(\mu_W)$ can be enhanced by large trilinear couplings T_{U33} and large Y_b for large $\tan\beta$ and large Y_t!

Benchmark scenario P1

Table 2: The MSSM parameters for the reference point P1 (in units of GeV or GeV^2 expect for $\tan\beta$). All parameters are defined at scale Q = 1 TeV, except $m_A(pole)$. The parameters that are not shown here are taken to be zero.

$\tan\beta$	M_1	M_2	M_3	μ	$m_A(pole)$
70	910	1970	2795	800	4970

$M^2_{\tilde{Q}22}$	$M^2_{\tilde{Q}33}$	$M^2_{\tilde{Q}23}$	$M^2_{\tilde{U}22}$	$M^2_{\tilde{U}33}$	$M^2_{\tilde{U}23}$
3630^2	3365^2	-740^2	2755^2	1510^2	-1705^2

$M^2_{\tilde{D}22}$	$M^2_{\tilde{D}33}$	$M^2_{\tilde{D}23}$	T_{U23}	T_{U32}	T_{U33}
2985^2	1270^2	-1820^2	2700	-260	4995

T_{D23}	T_{D32}	T_{D33}	T_{E33}
-2330	-335	3675	-335

$M^2_{\tilde{Q}11}$	$M^2_{\tilde{U}11}$	$M^2_{\tilde{D}11}$	$M^2_{\tilde{L}11}$	$M^2_{\tilde{L}22}$	$M^2_{\tilde{L}33}$	$M^2_{\tilde{E}11}$	$M^2_{\tilde{E}22}$	$M^2_{\tilde{E}33}$
4500^2	4500^2	4500^2	1500^2	1500^2	1500^2	1500^2	1500^2	1500^2

Current Constraints at 2 sigma level in the Re[C'$_7$(μ_b)/C$_7$(μ_b)]-Im[C'$_7$(μ_b)/C$_7$(μ_b)] plane

Constraints at 2σ
- $\mathcal{B}(B \to X_s\gamma)$
- $B^0 \to K^0_S\pi^0\gamma$
- $B^0_s \to \phi\gamma$
- $B^0 \to K^{*0}e^+e^-$
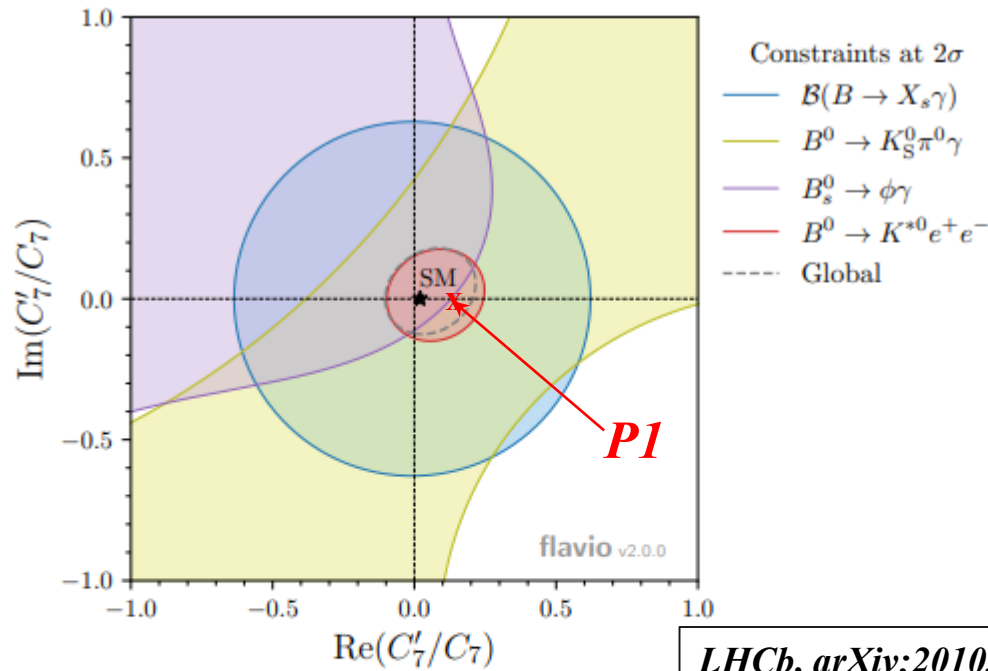- - - - - Global

P1

LHCb, arXiv:2010.06011

Figure 4: Constraints at 2σ level on the real and imaginary parts of the ratio of right- and left-handed Wilson coefficients, C'_7 and C_7. The C_7 coefficient is fixed to its SM value. The measurements of the inclusive branching fraction, $\mathcal{B}(B \to X_s\gamma)$, and the $B^0 \to K^0_S\pi^0\gamma$ mixing-induced CP asymmetry by the Belle and BaBar experiments [11–17] are shown in blue and yellow, respectively, the $B^0_s \to \phi\gamma$ measurements at LHCb [18] in purple and the measurement presented in this paper in red. The global fit is shown in dashed lines and the SM prediction is represented by a black star and corresponds to the ratio of s- and b-quark masses.

Benchmark point P1 is allowed by the current constraints including that from LHCb, arXiv:2010.06011!

Physical masses for the benchmark scenario P1

Table 3: Physical masses in GeV of the particles for the scenario of Table 2.

$m_{\tilde{\chi}_1^0}$	$m_{\tilde{\chi}_2^0}$	$m_{\tilde{\chi}_3^0}$	$m_{\tilde{\chi}_4^0}$	$m_{\tilde{\chi}_1^+}$	$m_{\tilde{\chi}_2^+}$
800	812	925	2030	809	2030

m_{h^0}	m_{H^0}	m_{A^0}	m_{H^+}
124.9	4970	4970	4997

$m_{\tilde{g}}$	$m_{\tilde{u}_1}$	$m_{\tilde{u}_2}$	$m_{\tilde{u}_3}$	$m_{\tilde{u}_4}$	$m_{\tilde{u}_5}$	$m_{\tilde{u}_6}$
2934	1231	2986	3431	3656	4491	4493

$m_{\tilde{d}_1}$	$m_{\tilde{d}_2}$	$m_{\tilde{d}_3}$	$m_{\tilde{d}_4}$	$m_{\tilde{d}_5}$	$m_{\tilde{d}_6}$
836	3272	3416	3654	4489	4492

$m_{\tilde{\nu}_1}$	$m_{\tilde{\nu}_2}$	$m_{\tilde{\nu}_3}$	$m_{\tilde{l}_1}$	$m_{\tilde{l}_2}$	$m_{\tilde{l}_3}$	$m_{\tilde{l}_4}$	$m_{\tilde{l}_5}$	$m_{\tilde{l}_6}$
1506	1507	1582	1495	1496	1509	1509	1564	1652

Flavor decompositions of the squark mass eigenstates for the benchmark scenario P1

Table 4: Flavour decompositions of the mass eigenstates $\tilde{u}_{1,2,3}$ and $\tilde{d}_{1,2,3}$ for the scenario of Table 2. Shown are the expansion coefficients of the mass eigenstates in terms of the flavour eigenstates. Imaginary parts of the coefficients are negligibly small.

	$\tilde{u}_L$	$\tilde{c}_L$	$\tilde{t}_L$	$\tilde{u}_R$	$\tilde{c}_R$	$\tilde{t}_R$
$\tilde{u}_1$	0	0.0016	0.0992	0	-0.4090	-0.9071
$\tilde{u}_2$	-0.0012	-0.0070	-0.0225	0	0.9104	-0.4130
$\tilde{u}_3$	0.0660	0.2921	0.9491	0	0.0607	0.0770

	$\tilde{d}_L$	$\tilde{s}_L$	$\tilde{b}_L$	$\tilde{d}_R$	$\tilde{s}_R$	$\tilde{b}_R$
$\tilde{d}_1$	0	0	0.0059	0	0.4057	0.9140
$\tilde{d}_2$	0	0.0059	0.0289	0	-0.9137	0.4054
$\tilde{d}_3$	0	0.2898	0.9566	0	0.0245	-0.0172

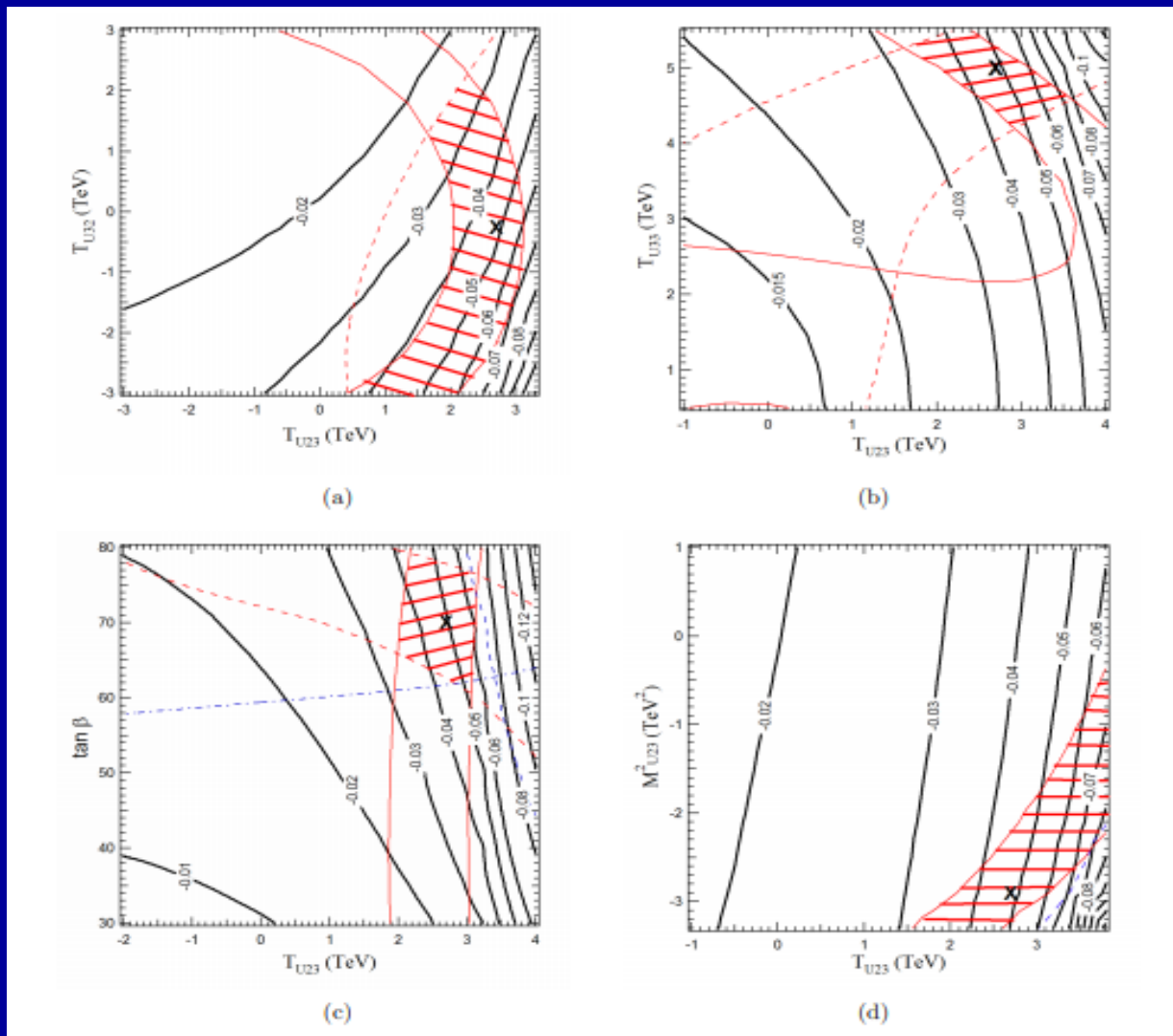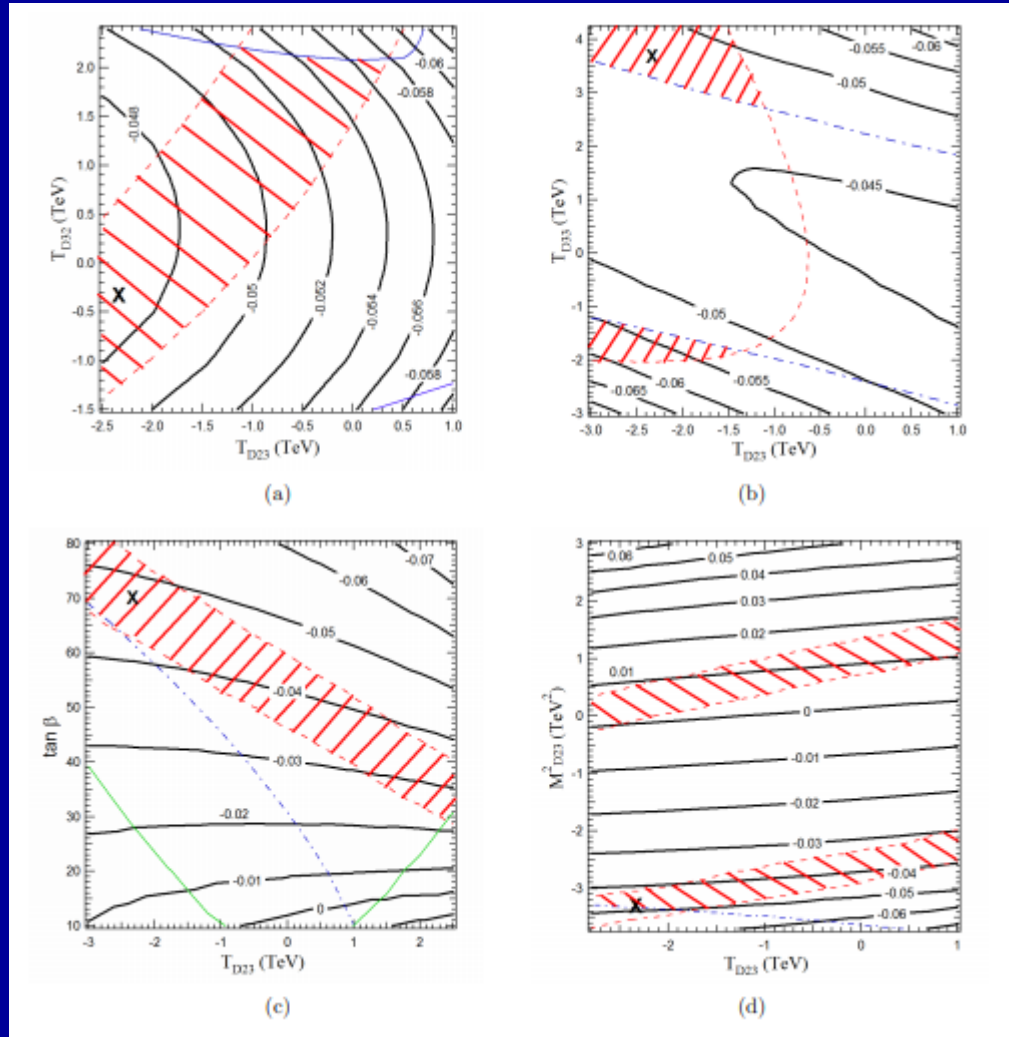# *Contour plots of the WCs around the benchmark point P1*

Figure 10: Contour plots of $Re(C'_7(\mu_b))$ around the benchmark point P1 in the parameter planes of (a) T_{U23} - T_{U32}, (b) T_{U23} - T_{U33}, (c) T_{U23} - $tan\beta$, and (d) T_{U23} - M^2_{U23}. The parameters other than the shown ones in each plane are fixed as in Table 2. The "X" marks P1 in the plots. The red hatched region satisfies all the constraints in Appendix A. The red solid lines, the blue dashed lines, the red dashed lines and the blue dash-dotted lines show the m_{h^0} bound, the B($b \to s\gamma$) bound, the B($B_s \to \mu^+\mu^-$) bound, and the $m_{\tilde{d}_1}$ bound, respectively.

Figure 11: Contour plots of $Re(C_7'(\mu_b))$ around the benchmark point P1 in the parameter planes of (a) T_{D23} - T_{D32}, (b) T_{D23} - T_{D33}, (c) T_{D23} - $tan\beta$, and (d) T_{D23} - M_{D23}^2. The parameters other than the shown ones in each plane are fixed as in Table 2. The "X" marks P1 in the plots. The red hatched region satisfies all the constraints in Appendix A. The definitions of the bound lines are the same as in Fig. 10. In addition to these the blue solid lines and the green solid lines show the ΔM_{B_s} bound and the vacuum stability bound on T_{D23}, respectively.
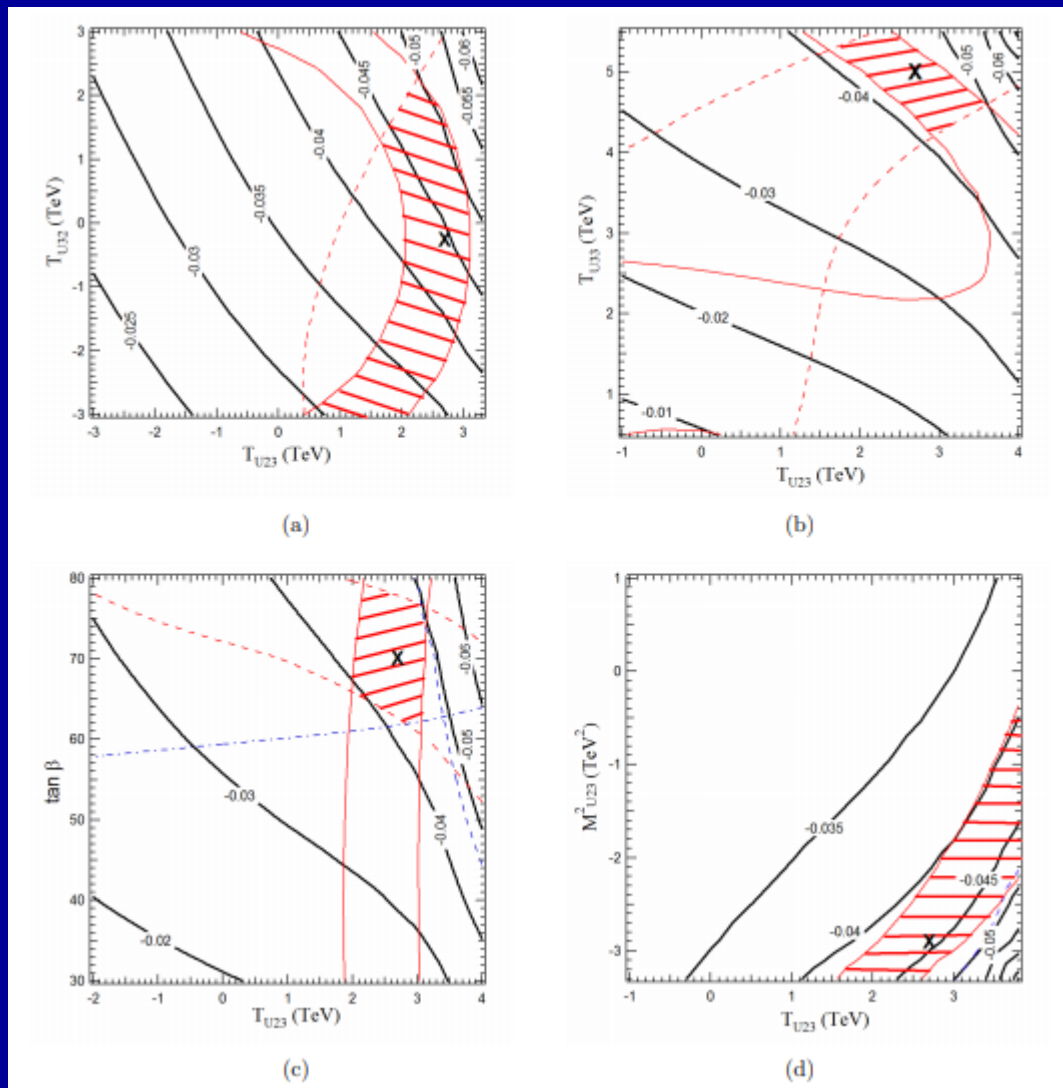
Figure 12: Contour plots of $Re(C_7^{\mathrm{MSSM}}(\mu_b))$ around the benchmark point P1 in the parameter planes of (a) T_{U23} - T_{U32}, (b) T_{U23} - T_{U33}, (c) T_{U23} - $tan\beta$, and (d) T_{U23} - M_{U23}^2. The parameters other than the shown ones in each plane are fixed as in Table 2. The "X" marks P1 in the plots. The red hatched region satisfies all the constraints in Appendix A. The definitions of the bound lines are the same as those in Fig. 10.
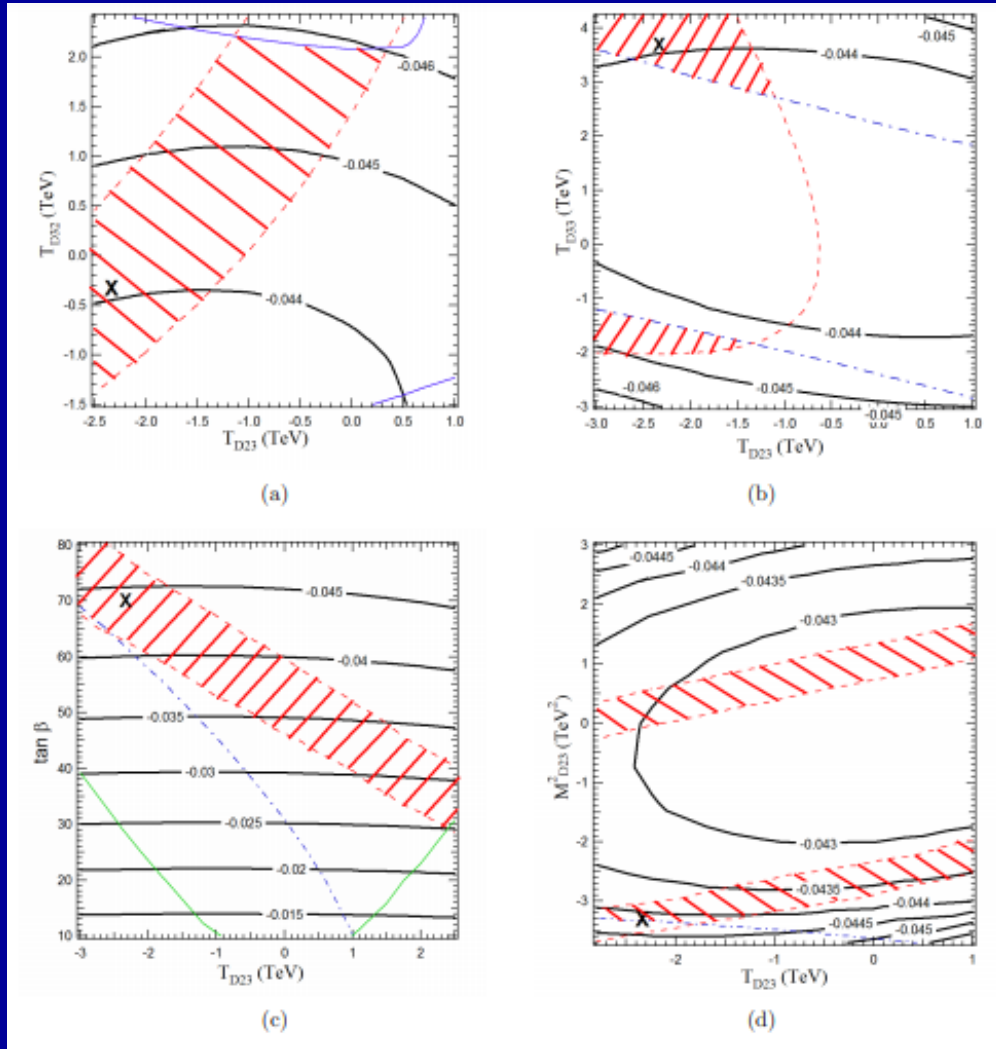
Figure 13: Contour plots of $Re(C_7^{\mathrm{MSSM}}(\mu_b))$ around the benchmark point P1 in the parameter planes of (a) T_{D23} - T_{D32}, (b) T_{D23} - T_{D33}, (c) T_{D23} - $tan\beta$, and (d) T_{D23} - M_{D23}^2. The parameters other than the shown ones in each plane are fixed as in Table 2. The "X" marks P1 in the plots. The red hatched region satisfies all the constraints in Appendix A. The definitions of the bound lines are the same as those in Fig. 11.